Australian National
University

Formation of the First Stars

Piyush Sharda

Panel: C. Federrath, M. Krumholz, M. Asplund, E. da Cunha

PhD Thesis Proposal
Research School of Astronomy and Astrophysics

June 2019

0

TABLE OF CONTENTS

1.0 INTRODUCTION

The formation and evolution of stars has been of interest to mankind for centuries. With the invention of telescopes with better resolution, wavelength coverage, sensitivity and throughput, it has become possible to observe and intricately study star-forming regions in the Milky Way and beyond. It is now well known that stars form from the collapse of molecular clouds composed mainly of neutral hydrogen. Stars are usually classified into three populations based on their metal content (Bond, 1981; McDowell, 1986). The generation of stars with the highest metallicity is known as Population I. Population II corresponds to stars that have relatively less metal content, and Population III is the hypothetical limit of stars that have no metals in them. Metal content also reflects formation time as a function of the age of the Universe. Population III stars are believed to have formed out of primordial species produced by the Big Bang, and hence have no metals in them. Population III is further classified into Population III.1 (the first generation of stars) and Population III.2 (primordial stars affected by radiation from other stars) (McKee and Tan, 2008; de Souza *et al.*, 2011). While current day star formation is well studied thanks to observations and simulations, the formation of the first generation of stars in the Universe still remains a mystery because of the lack of direct observations at spatially resolved scales beyond $z > 11.1$ (Oesch *et al.*, 2016), and the lack of surviving first stars in the Local Group (Griffen *et al.*, 2018; Hartwig *et al.*, 2019).

The first stars are believed to form between $15 \leq z \leq 30$, at the center of dark matter minihalos that have high baryonic densities (see reviews by Abel *et al.* 2002; Bromm and Larson 2004; Glover 2005; Ciardi and Ferrara 2005). As Figure 1 shows, the first molecular clouds of neutral hydrogen formed after the recombination of charged species (Peebles, 1968) by this epoch. These fragmented under the effects of self-gravity to give rise to the first stars.

Since the first clouds only contain primordial elements (H, He, Li and their isotopes), cooling during the collapse is highly inefficient as compared to current day star formation where dust, molecular line and metal line emissions can significantly increase the cooling rate (Omukai *et al.*, 2005). Figure 2 shows the evolution of temperature as a function of number density in collapsing clouds at different metallicities. As can be seen, the cooling becomes less and less efficient as the metallicity drops, thus the Jeans mass (a measure of the stability of the cloud against collapse, see Jeans 1902) increases. A primary issue that hinders our understanding of first stars formation is primordial chemistry. It is significantly different than the present-day star formation because of the presence of dust which is a more efficient radiator than molecules. Once the density gets high enough for the dust-gas collisional energy exchange to be efficient (above $\sim 10^{4.5}\,\mathrm{cm}^{-3}$), the dust completely controls the temperature, and the gas chemistry ceases to matter because molecular line emission is tiny compared to dust emission. Thus, although primordial chemistry is simpler, the chemical state of the gas should be treated as accurately as possible in primordial star formation. Hence, any simulation or modeling in the context of first stars usually needs an explicit chemical network that should be solved to evolve the collapse of the cloud.

Early simulations of the first stars were conducted at low resolution without accounting for all important physical processes. They formed only a single massive ($M > 100\,M_{\odot}$) central protostar, leading to the belief that the first stars were very massive and evolved in isolation (Bromm *et al.*, 2002; Abel *et al.*, 2002; Yoshida *et al.*, 2006; Glover and Jappsen, 2007), thus eliminating any chances of a pristine first star being alive to this date. The reason the first simulations of first stars did not exhibit fragmentation is that they did not include sink particles. Thus, they were either limited to very low resolution, or had to stop as soon as the first collapsed object formed. It was only once the simulations started using sink particles that they could run for thousands of years past the initial collapse. Since then, fragmentation has been observed in almost all simulations of the first stars. Moreover, it occurs very close to the central protostar, on scales as small as 1 AU (Klessen, 2018). This is because of the lack of an adiabatic core $>$ 1 AU even before protostar formation, as is observed in simulations of present day star formation (Larson, 1969; Bate, 1998). Thus, the circumstellar disk grows gradually and fragmentation occurs near the central protostar

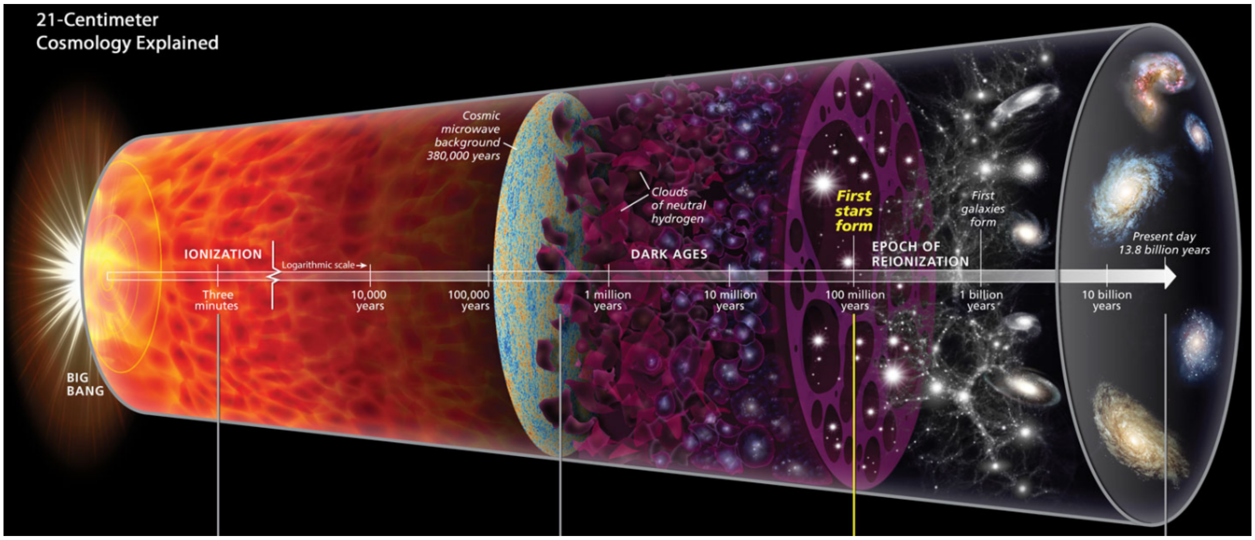

Figure 1: Figure taken from http://discovermagazine.com/~/media/Images/Issues/2014/April/21-centimeter-cosmology.jpg, depicting the epoch of the formation of the first stars in the cosmic context.

(Maki and Susa, 2004).

The observation that fragmentation occurs in simulations has encouraged discussions on the Initial Mass Function (IMF) of the first stars, which has emerged as a central goal of research on this topic. Understanding the IMF of the first stars is crucial to determining the metal enrichment of the Universe and photon budgets during the epoch of reionization (Sobral *et al.*, 2015; Xu *et al.*, 2016). It can also inform us about the nature of the first supernovae and black holes and help solve the mystery of supermassive blackholes observed in high-redshift galaxies (Fan, 2006; Omukai *et al.*, 2008; Silverman *et al.*, 2008; Tanaka and Haiman, 2009). The IMF is also important to understand the evolution of extremely metal-poor stars found in the Milky Way and nearby dwarf galaxies (Howes *et al.*, 2015; Frebel and Norris, 2015; Casey and Schlaufman, 2015). For a realistic simulation of first stars, one can take inspiration from cosmological simulations of the Universe that have successfully reproduced many of its large-scale properties (Springel, 2005; Vogelsberger *et al.*, 2013; Rocha *et al.*, 2013; Schaye *et al.*, 2015). Any realistic simulation of the first stars

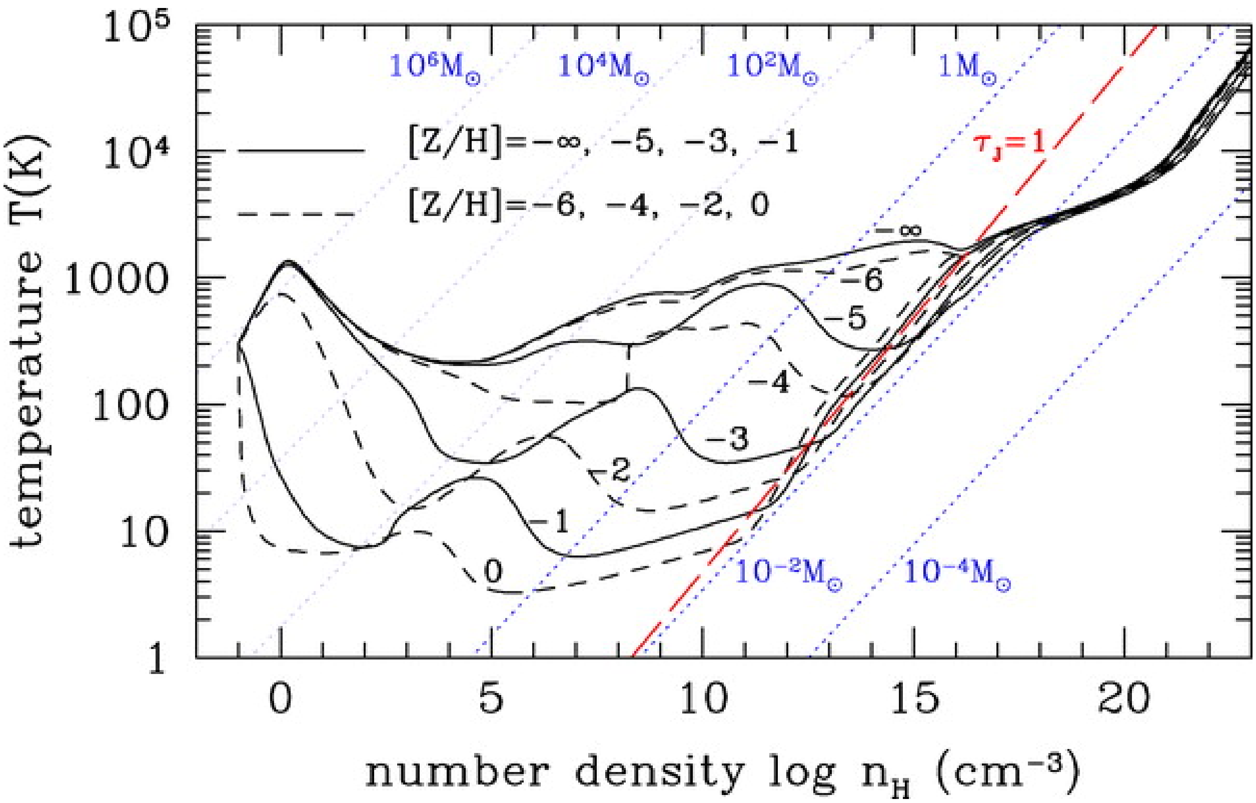

Figure 2: Figure adopted from Omukai *et al.* (2005), showing the 1-zone evolution of the temperature of star-forming clouds at different metallicities as a function of density after collapse sets in. Due to lack of efficient cooling pathways, first stars ($[Z/H] = -\infty$) are formed in primordial clouds that have higher Jeans mass compared to current day molecular clouds ($[Z/H] = 0$). The evolution is unaffected by chemistry once the high opacity continuum limit is reached ($\tau_{\mathrm{J}=1}$red-dashed line), and all tracks merge.

should be guided by initial conditions from such cosmological simulations together with the addition of key physical processes like primordial chemistry (Glover and Abel, 2008; Grassi *et al.*, 2014), turbulence (Clark *et al.*, 2011a; Turk *et al.*, 2012), magnetic fields (Machida *et al.*, 2008b; Schober *et al.*, 2012), dark matter annihilation (Smith *et al.*, 2012; Stacy *et al.*, 2014), primordial streaming velocities (Tseliakhovich and Hirata, 2010; Maio *et al.*, 2011) and radiation feedback (Hirano *et al.*, 2014, 2015; Hosokawa *et al.*, 2016). However, these simulations can only be followed up to a certain time after the collapse, before they become computationally expensive. Thus, they cannot yield a true distribution of the final population of first stars that forms within a reasonable computational time. Nonetheless, they can inform us about the earliest stages of primordial star formation that primarily set the mass distribution of the mature stellar population.

In addition to progress in simulations, high-resolution observational data is now becoming available through powerful and highly sensitive telescopes like the Atacama Large Millimetre/submillimetre Array (ALMA), Keck, the Australian Square Kilometre Array Pathfinder (ASKAP), and the Australia Telescope Compact Array (Wilson *et al.*, 2011). For indirect observational constraints on the first stars, we expect data from the James Webb Space Telescope (JWST), and from the near-future Giant Magellan Telescope (GMT), the European Extremely Large Telescope (E-ELT), Euclid, and the Wide-Field Infrared Survey Telescope (WFIRST) (Martell *et al.*, 2017). With these new surveys and observational facilities in place, the amount and detail of observational data will dramatically increase in the next 4 years, requiring dedicated modelling of the physical processes that give rise to the observations.

Table 1 summarises all 3D hydrodynamic simulations of first star formation published to date along with the physical processes they included. The time listed in the Table reflects that reached by the simulation after the formation of the first sink particle. AMR refers to adaptive mesh refinement, where the grid is adaptively refined (division of a parent cell into multiple child cells) or de-refined based on the density at a point (Berger and Colella, 1989), a method that is critical to following the collapse accurately in locations where the densities are high or high Mach number shocks are present. Chemistry is ticked 'Y' if the simulation used an explicit primordial chemical network together with the hydrodynamic module. Similarly, turbulence and magnetic fields, if included in any form in the simulation, are marked as 'Y' in the respective row. There are many types of radiation feedback that should be considered for simulations of primordial star formation, for example, that from Lyman-Werner photons, cosmic rays, jets/outflows, etc. If any one of these feedback processes are included in the simulation, the column entry is 'Y'.

The simulations that have been done over the last two decades cover a wide range of parameter space in terms of resolution (hence, density) and time period. A common feature in all these simulations is the formation of a central protostar. We notice that most of these simulations do not work with an adaptive grid that can be refined as the density increases and more resolution is required to resolve the small-scale structures. While the nested grid or particle based codes have certain advantages over an adaptive mesh refinement (AMR) based grid, they may not resolve the regions where high velocity shocks are present, for example, near the edge of accretion discs of protostars (Plewa, 2001; O'Shea *et al.*, 2005; Hubber *et al.*, 2013a). Further, the chemical networks have been periodically updated every few years with more accurate rate constants and enthalpies, which can have significant effects on the evolution of the system. Thus, it becomes clear that there are many areas where we can contribute to the ongoing research on first stars. In this project, we plan to use an AMR MHD code to simulate the collapse of primordial clouds at high resolution, under the effects of turbulence and magnetic field structures together with accurate thermodynamic treatment of primordial species and radiation feedback.

Table 1: Summary of all 3D MHD simulations of the first stars. Columns III and IV denote the maximum density reached and time after the first sink formed in the simulation.

S. No.	Work	Max Density cm^{-3}	Time yr	AMR	Chemistry	Turb	Mag Fields	Rad Feedback	Disk Frag
1	Abel *et al.* (2002)	10^8	−−	N	Y	N	N	N	N
2	Bromm *et al.* (2002)	10^{14}	−−	Y	Y	N	N	N	N
3	Saigo *et al.* (2004)	10^{20}	200	N	N	N	N	N	Y
4	Yoshida *et al.* (2006)	10^{15}	−−	N	Y	N	N	N	N
5	Gao *et al.* (2007)	10^{11}	−−	N	Y	N	N	N	N
6	O'Shea and Norman (2007)	10^{15}	200000	Y	Y	N	N	N	N
7	Machida *et al.* (2008b)	10^{22}	3000	N	N	N	N	N	Y
8	Machida *et al.* (2008a)	10^{22}	0.4	N	N	N	Y	N	N
9	Turk *et al.* (2009)	10^{16}	200	Y	Y	N	N	N	Y
10	Stacy *et al.* (2010)	10^{12}	5000	N	Y	N	N	N	Y
11	Stacy *et al.* (2011)	10^{12}	5000	N	Y	N	N	N	Y
12	Hosokawa *et al.* (2011)	10^{12}	13000	N	Y	N	N	Y	Y
13	Greif *et al.* (2011)	10^{16}	1000	N	Y	N	N	Y	Y
14	Clark *et al.* (2011a)	10^{12}	3000	N	Y	Y	N	N	Y
15	Stacy *et al.* (2012)	10^{12}	5000	N	Y	N	N	Y	Y

16	Greif *et al.* (2012)	10^{19}	10	N	Y	N	N	N	Y
17	Turk *et al.* (2012)	10^{14}	$--$	Y	Y	Y	Y	N	Y
18	Susa (2013)	10^{13}	10^{5}	N	Y	N	N	Y	Y
19	Machida and Doi (2013)	10^{18}	1000	N	Y	N	Y	N	Y
20	Stacy and Bromm (2014)	10^{16}	5000	N	Y	N	N	Y	Y
21	Susa *et al.* (2014)	10^{12}	10^{5}	N	Y	N	N	Y	Y
22	Hirano *et al.* (2014)	10^{12}	5000	N	Y	N	N	Y	Y
23	Hummel *et al.* (2015)	10^{12}	5000	N	Y	N	N	Y	Y
24	Hummel *et al.* (2016)	10^{12}	5000	N	Y	N	N	Y	Y
25	Latif and Schleicher (2016)	10^{16}	40	Y	Y	Y	N	N	Y
26	Stacy *et al.* (2016)	10^{16}	5000	N	Y	N	N	Y	Y
27	Hirano and Bromm (2017)	10^{15}	10^{5}	N	Y	N	N	N	Y
28	Hirano *et al.* (2018)	10^{12}	5000	N	Y	N	N	N	Y

2.0 RESEARCH PROPOSAL

One of the primary objectives of this research is to advance our understanding of the IMF of the first stars and how the IMF influences the subsequent evolution of the large-scale Universe and next generation(s) of star formation. We aim to study the formation and evolution of systems bearing first stars through 3D MHD simulations using the grid-based AMR code FLASH (Fryxell *et al.*, 2000; Dubey *et al.*, 2008) where we can refine and derefine regions in the simulation based on the Jeans length which characterizes the collapse of a system. Table 2 shows my supervisory panel with their key expertise relevant to this project. This research forms a part of the Australian Research Council Future Fellowship on Formation of the First Stars (`FT180100495`; PI: Federrath). With the available computational time on the NCI supercomputer Raijin through projects `ek9` (PI: Federrath), `jh2` (PI: Krumholz) and `iv23` (PI: Power), we aim to carry out multiple realizations of my simulations at different resolutions. This will not only help build a statistical population of first stars and study their distributions, but also prove useful to check numerical convergence and report the effects of grid noise and limited resolution. The different sections in this chapter present my detailed working plan on including the different key physical processes in the simulations.

2.1 PRIMORDIAL CHEMISTRY

One of the key physical differences between primordial and present-day star formation is the absence of metals and the inefficient formation of molecules in the absence of dust, during the evolution of the star-forming halos. As a result, primordial halos cool inefficiently due to the absence of metal line emission. Thus, any simulations of first stars formation should

Table 2: Supervisory Panel. * Primary/Chair

S. No.	Designation	Name	Expertise
1.	Assoc. Prof.	Christoph Federrath*	Star Formation Theory/Simulations
2.	Prof.	Mark Krumholz	Star Formation Theory/Simulations
3.	Prof.	Martin Asplund	Metal-Poor Stars and Stellar Evolution
4.	Dr.	Elisabete da Cunha	High-Redshift Universe

include a systematic thermochemical treatment by taking into account the relevant chemical reactions of primordial species like H, H_2, HD, etc., and the physical processes that govern the evolution of temperature and density.

We plan to utilize the KROME[1] package for primordial chemistry that has been developed for astrophysical applications (Grassi *et al.*, 2014). KROME uses a subroutine of predesigned (re-writable) chemical networks for various astrophysical phenomena that can be embedded in numerical codes like FLASH. It uses the ODE solver `DLSODES`[2] to solve the reaction network and evolve the temperature and density of the system in accordance with the chemistry and the specified heating/cooling processes (Grassi *et al.*, 2013; Bovino *et al.*, 2013). The network of primordial chemical reactions we will utilize in our simulations is `react_primordial_wD` which includes reactions between the following species: H, H_2, HD, H^+, H^-, D, D^+, D^-, He, He^+, He^{++}, H_2^+ and HD^+. Although Big-Bang nucleosynthesis also produced some minute quantities of Li (Fields, 2011), it has been shown that chemical reactions involving Li or its ionized forms have negligible effects on the evolution of the system due to low abundances and reaction rates (Lepp and Shull, 1984; Galli and Palla, 2013). The reactions included in the package have been taken from various works, either directly, or by fitting the reaction coefficients as obtained from observations (Aldrovandi and Pequignot, 1973; Mitchell and Deveau, 1983; Janev *et al.*, 1987; Dalgarno and Lepp, 1987;

[1] http://www.kromepackage.org/

[2] http://www.radford.edu/~thompson/vodef90web/

Cen, 1992; Verner and Ferland, 1996; Abel *et al.*, 1997; Stancil *et al.*, 1998; Galli and Palla, 1998; Omukai, 2001; Galli and Palla, 2002; Savin *et al.*, 2004; Yoshida *et al.*, 2006; Capitelli *et al.*, 2007; Glover and Abel, 2008; Glover and Savin, 2009; Stenrup *et al.*, 2009; Kreckel *et al.*, 2010; Glover *et al.*, 2010; Coppola *et al.*, 2011; Forrey, 2013).

The cooling processes we will include are: 1.) cooling by molecular hydrogen which is important at both low and high densities, 2.) collisionally induced emission (CIE) cooling due to supermolecular structures at high densities, 3.) cooling due to chemical reactions, 4.) cooling due to HD formation, 5.) atomic cooling which is dominant at high temperatures and 6.) cooling due to Compton scattering of cosmic microwave photons by free electrons. At high densities, a term to account for opacity should be included in the cooling process because the gas becomes optically thick. For this purpose, we plan to utilize the H_2 cooling function defined by Ripamonti and Abel (2004) which includes a treatment for opacity. However, this approximation diverges from the more detailed treatment of opacity conducted by Hirano and Yoshida (2013) when the molecular fraction of Hydrogen is less than ~ 0.5. Nonetheless, this should not have a big impact on the simulation since the chemistry in cells where the mass fraction of H_2 is not abundant is controlled by H. The heating processes we include are the 1.) chemical heating generated from reaction enthalpies and 2.) compressional heating set by the hydrodynamics module `Bouchut` (Bouchut *et al.*, 2007, 2010; Waagan *et al.*, 2011).

2.1.1 Thermodynamics of H_2

The adiabatic index (γ) determines how easy or hard it is to compress the gas, and thus how much the gas resists fragmentation. A gas with higher γ is more resistant to fragmentation because, for the same level of pressure fluctuation, it will respond with a smaller density fluctuation than a gas with lower γ (Boley *et al.*, 2007). Given that the formation of first stars depends sensitively on the chemistry of H_2, it is important to treat its thermodynamics H_2 as accurately as possible. In the context of present day star formation, the adiabatic index of H_2 can be assumed to be constant because the temperatures are low enough that the rotational or vibrational degrees of freedom are not excited[3]. Thus, in such simplified

[3]Only valid during the collapse phase. Inner accretion discs around present day protostars can have temperatures > 100 K where the adiabatic index of H_2 cannot be assumed to be a constant similar in

limits, H_2 can be considered as a monoatomic gas ($\gamma_{H_2} = 5/3$) or a diatomic gas ($\gamma_{H_2} = 7/5$) depending on the available degrees of freedom. However, because the formation of the first stars takes place in primordial clouds at temperatures of a few 100 K, the adiabatic index for H_2 cannot be treated as constant. It depends on the temperature and the ratio of ortho to para H_2 (which are the two nuclear spin orientations of the molecule, see Matthews *et al.* 2011). The continuum limit does not apply because the levels are not closely spaced, requiring a quantum mechanical treatment. Figure 3 shows the variation of the adiabatic index of the system as a function of temperature at different mass fractions of H_2. We describe the detailed calculation in Appendix A.

Following Figure 3 and Appendix A, it becomes evident that H_2 can be approximated as a monoatomic gas at low temperatures ($T < 50$ K) and a diatomic gas at high temperatures where the continuum limit is reached ($T > 10000$ K). Primordial star formation sits squarely in between these two regimes. Thus, by properly incorporating variation of the adiabatic index as a function of temperature, we will be able to study and compare fragmentation in primordial discs where γ_{H_2} is taken to be a constant ($\gamma_{H_2} = 7/5$), the assumption used in all previous published work, to the results when it is calculated as a function of temperature. Some work on this has been done in the past (Omukai and Nishi, 1998), but only in a 1D model where fragmentation is of course impossible.

The key additions from this research to the field of primordial thermochemistry in metal-poor environments are:

1. The effects of different heating and cooling processes on the collapse of primordial clouds.
2. Fragmentation in primordial discs in the presence of accurate thermodynamic treatment of molecular hydrogen.

2.2 ROLE OF TURBULENCE AND MAGNETIC FIELDS

We find from Table 1 that most simulations of first stars done to date lack turbulence and/or magnetic fields. This is attributed to the highly unconstrained primordial magnetic

shocked gas; for example, protostellar jet-shocked gas.

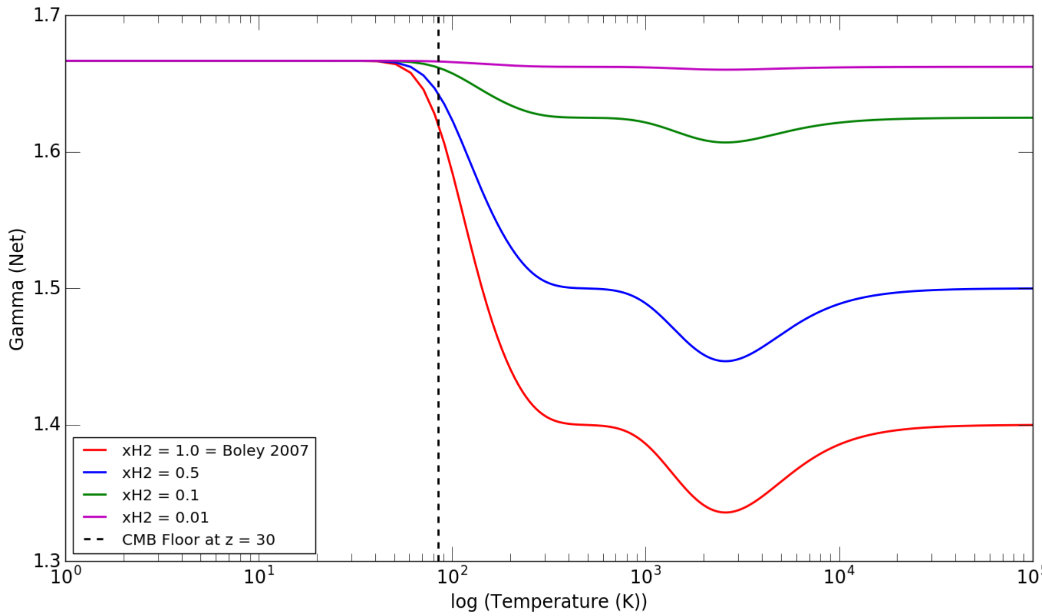

Figure 3: The adiabatic index of a system consisting of primordial species, with different mass fractions of H_2 (x_{H_2}) as a function of temperature (Sharda et al. 2019a, in prep.). Because the adiabatic index varies as a function of temperature in the parameter space of interest for primordial cloud collapse, it is important to treat the degrees of freedom of H_2 accurately.

field strength, with values ranging around 1nG − 1fG (Kahniashvili *et al.*, 2013, 2014; Saga *et al.*, 2018; Cheera and Nigam, 2018). The quiescent early Universe has been conventionally assumed to be largely non-turbulent (Gibson, 1996). However, once high-density baryonic regions are created in dark matter minihalos and begin to collapse, gas is driven to the center of these regions at high velocities. The Reynolds numbers of the resulting flows are very large, favouring the development of turbulence. Moreover, the streaming velocities between the dark matter and baryons can also contribute to turbulence (Fialkov *et al.*, 2014). Further, even a small amount of seed turbulence can amplify the magnetic fields to large values through small-scale dynamo action (Brandenburg and Subramanian, 2005; Federrath *et al.*, 2011; Brandenburg *et al.*, 2012; Schober *et al.*, 2012; Federrath *et al.*, 2014). Hence, it is vital to understand how turbulence acts during the formation of the first stars and modulates the magnetic field strength during collapse.

Numerous studies have shown that it is important to resolve the scales at which turbulence can amplify magnetic fields through the dynamo action. It is common to use the Truelove criterion for refinement in gravito-hydrodynamic simulations, which requires at least 4 cells per Jeans length to resolve the ongoing collapse of the system (Truelove *et al.*, 1997). However, Federrath *et al.* (2011) showed that one needs at least 32 cells per Jeans length to resolve the scales at which turbulence can amplify magnetic fields (see Figure 4, Sur *et al.* 2010). In fact, using less than ~30 grid cells per Jeans lengths leads to underestimates not only in the amplification, but also in the amount of kinetic energy that is resolved on the Jeans scale (Federrath *et al.*, 2011) and the structure of the gas (for example, the scale height of accretion discs; see (Federrath *et al.*, 2014)). Such a large difference in the refinement criteria is already a major improvement over other simulations that we plan to implement.

It is well known that simulations cannot reproduce realistic Reynolds numbers found in turbulent environments in the primordial Universe, which are of the order of 10^6 (Schober *et al.* 2012; see also, Haugen *et al.* 2004; Kitsionas *et al.* 2009). In the ideal case of infinite resolution, one would expect to see magnetic fields eventually saturate as turbulence converts kinetic energy into magnetic energy. Sur *et al.* (2014) showed that even a weak turbulent seed can saturate the magnetic fields on timescales smaller than the free-fall timescale of collapse. We can achieve this by introducing a saturated magnetic field in the `StirICs` module in FLASH in our simulations. This will allow us to perform a parameter study of the effects of different magnetic field strengths during the onset of collapse in primordial clouds.

To analyze the type and nature of outflows from the first protostars, we intend to use the `SinkOutflow` module in FLASH's sink particle module which can trace the amount of mass being ejected by the protostar and its variation as a function of the orientation and structure of the initial magnetic field, by the advection of mass scalars in the system. It is well known that an ordered component of magnetic field can lead to the launching of jets and outflows from a system undergoing rotational motion (Pudritz and Norman, 1986;

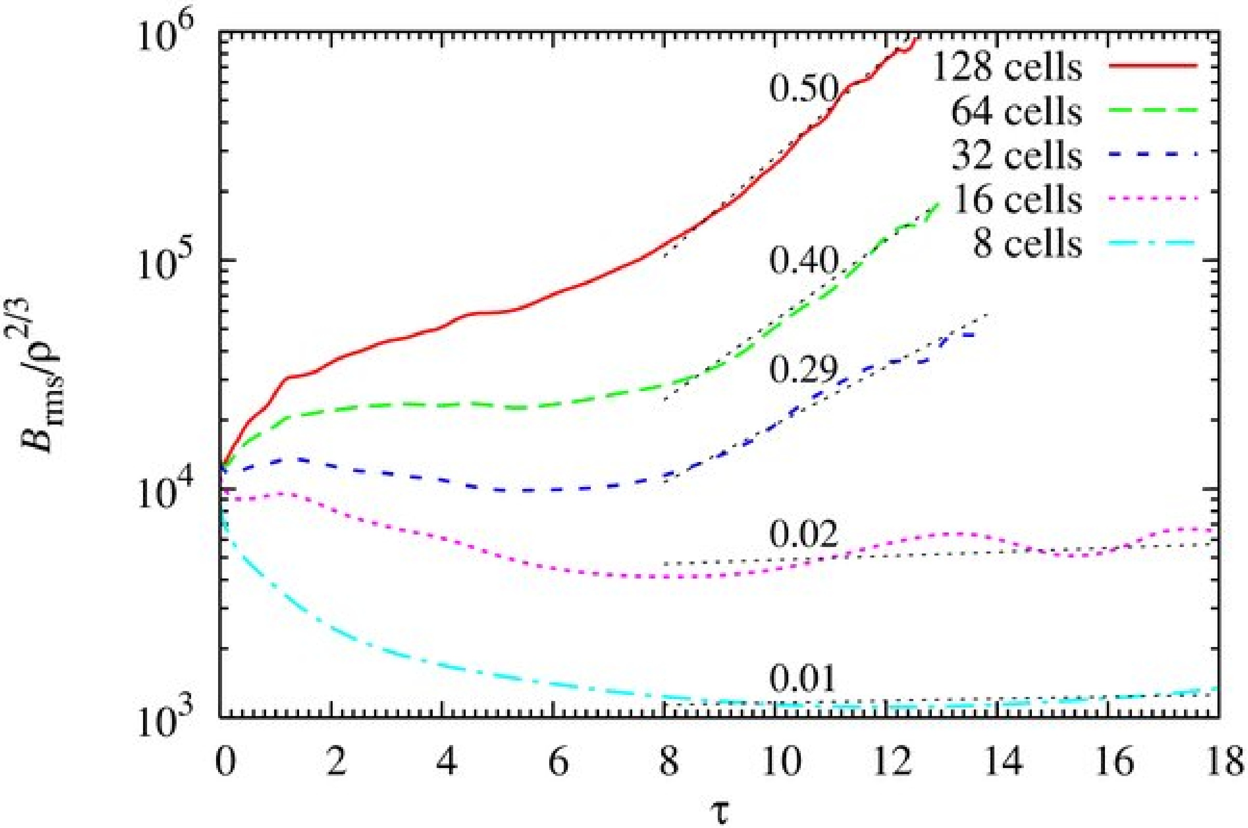

Figure 4: Figure adopted from Federrath *et al.* (2011), showing the evolution of the rms component of magnetic field (or, the turbulent magnetic field) relative to the amplification by compression of the field ($\rho^{2/3}$) of star-forming clouds at different times during collapse. At least 32 cells per Jeans length are required to resolve the small-scale turbulence that can amplify the magnetic fields through the dynamo action (Brandenburg and Subramanian, 2005). This is 8× better resolution than is usually adopted for simulations of cloud collapse based on the Truelove criterion for resolving the Jeans length (Truelove *et al.*, 1997).

Crutcher, 1999; Wu *et al.*, 2004; Banerjee and Pudritz, 2006; Price and Bate, 2007). Gerrard *et al.* (2019) recently carried out a study on outflows in the presence of different types of magnetic fields (ordered, mixed and turbulent; see Figure 5) in the context of present day star formation. As we see from Figure 6, different magnetic field geometries have a significant impact on the distribution of the underlying stellar population and thus may play a crucial role in determining the IMF. Given the highly turbulent flow in dark matter minihalos, the fields will be completely tangled up very quickly and there may not be an ordered component present. However, if the $\alpha\omega$ dynamo works, it can generate and sustain an ordered component (Pariev and Colgate, 2007; Pariev *et al.*, 2007). This is so because the $\alpha\omega$ dynamo can transfer magnetic energy back and forth between different directions. Further, even a magnetic field that is un-ordered on large scales will be ordered if looked at on sufficiently small scales. Hence, we plan to conduct a similar analysis of the dependence on field geometry for a fiducial magnetic field strength in a primordial cloud, as done for present day star formation. Based on the conclusions of previous works investigating the dependence of magnetic energy on the turbulent Mach number and magnetic Prandtl number[4] of the gas (Federrath *et al.*, 2011, 2014; Schober *et al.*, 2015), we plan to perform a parameter study of the magnetic field strength at sonic Mach numbers and high Prandtl numbers which are expected in the early Universe at the onset of the collapse of primordial clouds (Brandenburg and Subramanian, 2005; Greif *et al.*, 2008; Clark *et al.*, 2011b).

In summary, the key additions from this research to the broad fields of turbulence and magnetic fields in first stars and the early Universe can be:

1. The effects of turbulence on first star formation.

2. Studies of resolved magnetic fields emerging from small seeds through the dynamo action.

3. Studies of ordered and unordered components of magnetic fields and their role in disk fragmentation and outflows/jets.

[4]Magnetic Prandtl number is the ratio of viscosity to magnetic diffusivity.

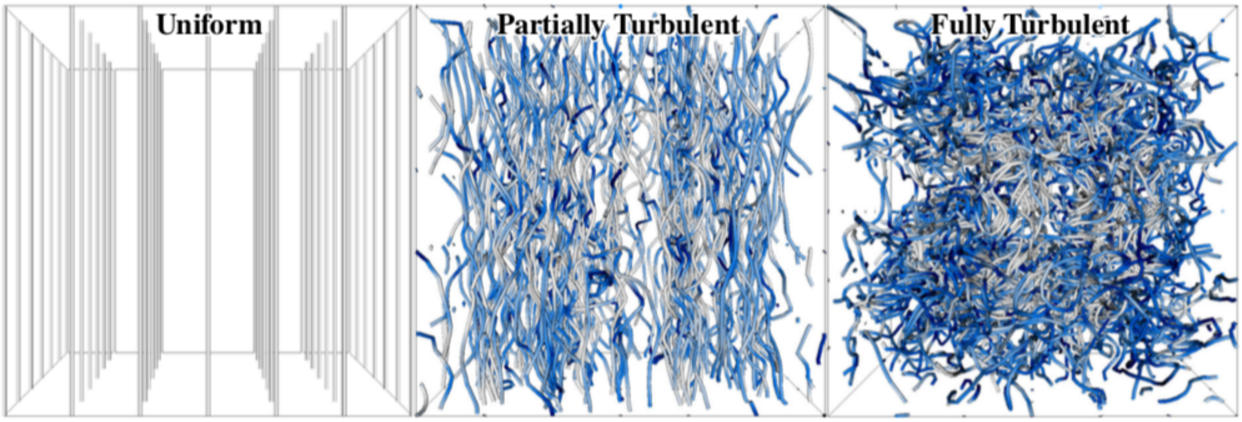

Figure 5: Figure adopted from Gerrard *et al.* (2019), showing the different magnetic field structures we plan to introduce in my simulations to study the effects of magnetic field geometry on first star formation.

2.3 POST COLLAPSE STUDIES

2.3.1 Sink Mass Distribution and Multiplicity

Sink particles are frequently used in hydrodynamic simulations of star formation as a proxy for stellar sources. These Lagrangian particles can travel inside the grid, accrete gas from it and alter the local gravitational potential in the region. We intend to use the `Sink` particle module in FLASH to track the evolution of overdense regions in the simulation which will eventually form protostellar cores (Federrath *et al.*, 2010). FLASH uses a rigorous set of checks to ensure that bound and collapsing mass in regions crossing the density threshold at the highest level of refinement is converted into a sink while avoiding artificial fragmentation. Invented by Bate *et al.* (1995), sink particle techniques have been extensively employed in both AMR and smoothed particle hydrodynamics (SPH) MHD simulations of star formation (Krumholz *et al.*, 2004; Jappsen *et al.*, 2005; Wang *et al.*, 2010; Padoan and Nordlund, 2011; Gong and Ostriker, 2013; Hubber *et al.*, 2013b; Bleuler and Teyssier, 2014; Jones and Bate, 2018).

We plan to use the sink particle module in FLASH as a substitute for stellar sources in our

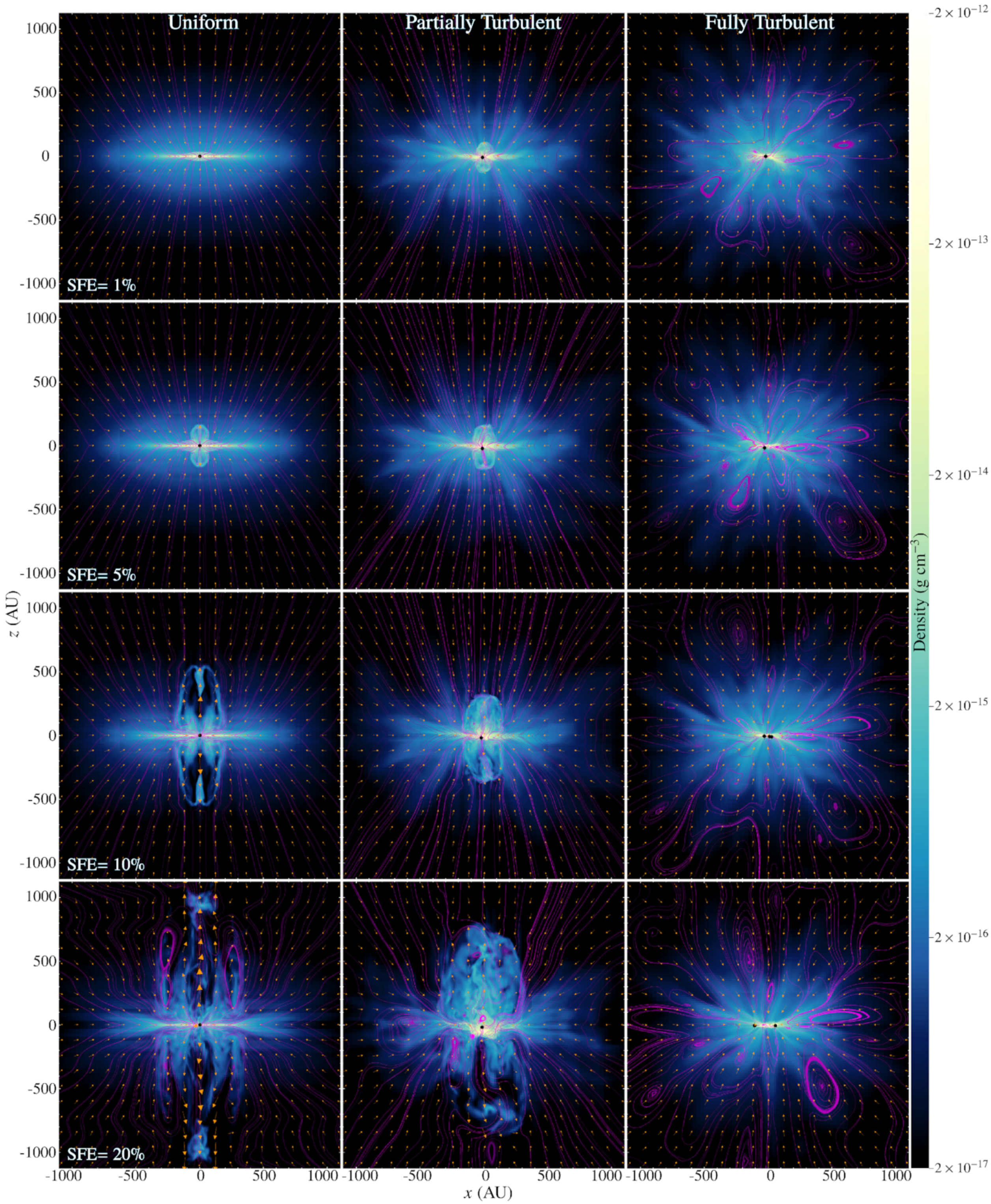

Figure 6: Figure adopted from Gerrard *et al.* (2019), showing the origin of protostellar outflows with different magnetic field structures.

simulations. The distribution of sink masses will thus be a crucial information to comment on the fragmentation of primordial discs under different physical processes. By following the algorithm used in Krumholz *et al.* (2012b) that calculates the number of bound sinks in a binary, triple or quadruple network, we also plan to investigate the multiplicity fraction in these systems, which we expect to be high given that fragmentation occurs close to the primary star which will result in closely bound systems.

2.3.2 Accretion Characteristics of First Stars

The number and masses of sink particles that form in the simulation is a direct measure of fragmentation properties of the primordial disk, which can inform us about the nature of the mass function of the first stars. We plan to study the star formation efficiency of the different primordial clouds we will simulate as the ratio of the mass in sink particles at a time over the total initial mass of the cloud. While this empirical estimate of the star formation efficiency needs a more complex treatment if it were to be compared with that for current day (or, low-redshift) star formation, it is a useful tool to characterize the system. Based on the amount of mass accreted by a sink, its luminosity and temperature will vary which will be important for the radiation feedback mechanism that may limit further fragmentation (Guszejnov *et al.*, 2018).

2.3.3 Realistic Primordial Cloud Geometries

We will initiate our simulations by setting up a spherical cloud core with a homogeneous density. Taking inspiration from cosmological simulations that form dark matter minihalos where baryonic cores form in overdense regions, we define the core mass $M_{\rm core} = 1000\,M_\odot$ and radius $R_{\rm core} = 1\,\rm pc$. These parameters are similar to that for Bonnor-Ebert spheres on the verge of collapse, which are often used in such simulations as initial conditions (Turk *et al.*, 2012; Hummel *et al.*, 2015; Schaye *et al.*, 2015; Hirano *et al.*, 2018). Our initial density ($n_{\rm core} = 9050\,\rm cm^{-3}$) is thus in good agreement with the overdensity observed in cosmological simulations (Hirano *et al.*, 2015). Based on 1D calculations of primordial cloud collapse using KROME that we run from low densities ($n = 1\,\rm cm^{-3}$), we find that the temperature reaches

270 K by the time $n \sim 10^4\,\mathrm{cm}^{-3}$. Thus, we set $T_{\rm core} = 270\,\mathrm{K}$. To ensure the simulation box is in pressure equilibrium, we set the corresponding background density and temperature to be 100 times lower and higher, respectively. We set the initial angular velocity of the core such that the rotational energy is 3 per cent of the gravitational energy. This choice is motivated by the angular momentum of minihalos observed in cosmological simulations (Druschke *et al.*, 2018) and the formation of disc around the protostars in present-day star formation simulations (Burkert and Bodenheimer, 2000; Lewis and Bate, 2018).

After performing the initial set of simulations for a homogeneous and spherical primordial cloud core, we plan to use more realistic geometries of primordial clouds. For this purpose, we plan to use cosmological simulations like ILLUSTRIS TNG (Marinacci *et al.*, 2018) or EAGLE (Schaye *et al.*, 2015) where the resolution is sufficient to resolve the dark matter mini-halos where the first stars eventually form. Such zoom-in techniques have been used to demonstrate the diversity of first star halos one can obtain (Becerra *et al.*, 2015; Hirano *et al.*, 2015). Based on the rotational velocity and structural variations of the halo (see Figure 7), we expect to find differences in the rate of collapse and fragmentation in primordial discs. The initial structure and spin of the halos largely define the angular momentum transport in the cloud (Teklu *et al.*, 2015; Druschke *et al.*, 2018). In fact, it has also been proposed that the spin will also affect the magnetic field strength in the clouds (Hirano *et al.*, 2018). Such an analysis can be carried out multiple times for different minihalo geometries by changing the initial seed of turbulence, thus generating a statistical population of first stars that is not biased by random fluctuations.

In summary, the key additions from this research to the field of early Universe cosmology and structure formation can be:

1. Turbulent fragmentation of magnetized primordial clouds extracted from cosmological minihalos.

2. Statistical treatment of the mass distribution of the first stars in resolved 3D MHD simulations.

3. The effects of angular velocities of dark matter minihalos on the formation of the first stars.

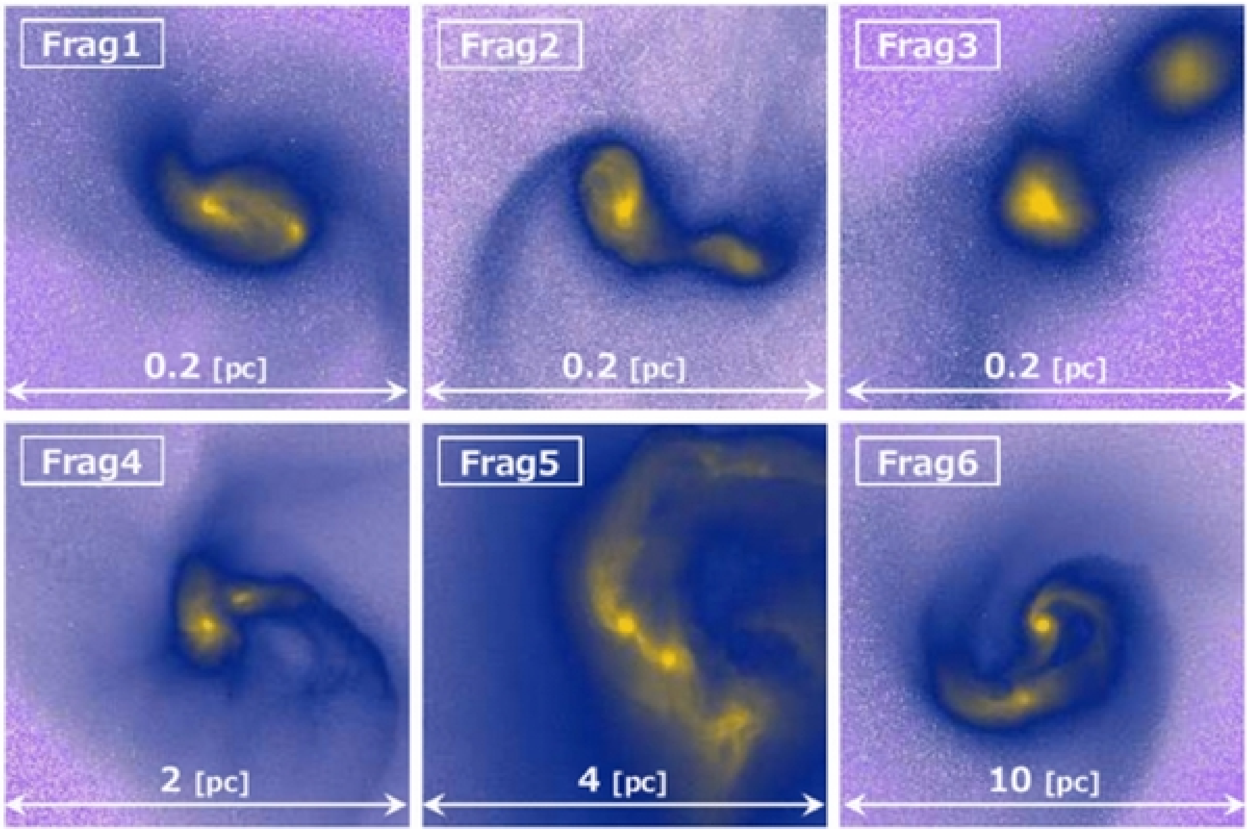

Figure 7: Figure adopted from Hirano *et al.* (2014), showing the different structures of clouds formed in cosmological simulations based on the spin of minihalos. The non-symmetrical shape and the corresponding presence of density fluctuations in these halos may have a significant effect on the collapse of the primordial clouds and the subsequent fragmentation of primordial discs.

2.4 RADIATION FEEDBACK

It is vital to include a treatment of the different radiative processes that occur in star-forming clouds, because they can significantly influence the final masses and dynamical interactions of stars in a cluster. In the primordial case, it has been shown that radiation feedback can halt the growth of a protostar beyond $M_\star > 30 M_\odot$ (see Figure 8, adopted from Hosokawa *et al.* 2011). In this project, we plan to work on two key radiation feedback processes which play an important role in the formation of the first stars.

We plan to include the effects of Lyman-Werner photons on primordial minihalos in my simulations. These photons have energies $11.2 < h\nu < 13.6\,\mathrm{eV}$ and are capable of photo-dissociating H_2 which is the primary coolant in primordial gas at high densities (Allison and Dalgarno, 1969). They are produced from massive protostars and can escape their host minihalos. This effect can create a LW photon background, whose strength depends on the escape fraction, which can dissociate H_2 in minhalos that have not yet collapsed, thus affecting their star formation process (Schauer *et al.*, 2017; Regan and Downes, 2018). To approximate the self-shielding factor, we plan to estimate the column density of H_2 in our simulations with the ray-tracing module recently developed for FLASH (Buntemeyer *et al.*, 2016). Using the self-shielding factor, one can then find out the rate of dissociation of H_2 and treat this as a chemical reaction along with the primordial network present in Krome. Following Draine and Bertoldi (1996), the H_2 dissociation rate can be written as

$$k_{\mathrm{H_2}} = 1.1 \times 10^8 f_{\mathrm{shield,H_2}} \mathrm{s}^{-1}\,, \tag{2.1}$$

where $f_{\mathrm{shield,H_2}}$ is the self-shielding factor for H_2, which can be estimated (for the case where there is no dust) as

$$f_{\mathrm{shield,H_2}} = \frac{0.965}{(1+x/b_5)^a} + \frac{0.035}{(1+x)^{0.5}} \exp(-8.5 \times 10^{-4}(1+x)^{-0.5})\,, \tag{2.2}$$

where $x = N_{\mathrm{H_2}}/5 \times 10^{14}\,\mathrm{cm^{-2}}$ represents the column density of H_2 and $b_5 = b/10^5\,\mathrm{cm\,s^{-1}}$ represents the Doppler broadening parameter of the gas, given by $b = \sqrt{kT/m_{\mathrm{H}}}$. a is a constant which was recently refined to be 1.1 by Wolcott-Green *et al.* (2011) based on the results from their numerical radiative transfer calculations. Similarly, the shielding factor for H can be defined as (Schauer *et al.*, 2015)

$$f_{\mathrm{shield,H}} = \frac{1}{(1+x_{\mathrm{H}})^{1.62}} \exp(-0.149\, x_{\mathrm{H}})\,, \tag{2.3}$$

The ray-tracing module can directly measure the column density of H_2, and thus, x. The Doppler broadening factor must include both thermal and turbulent broadening, since both microscopic and bulk motion can shift molecules out of resonance with Lyman-Werner photons. We plan to include the contribution of turbulent motions to Doppler broadening, which has not been investigated in primordial star formation and has been shown to be crucial to constraining the escape fraction near the Epoch of Reionization (Safarzadeh and Scannapieco, 2016) given the high turbulence observed in high-redshift galaxies (Sharda *et al.*, 2018; Sharda *et al.*, 2019). This treatment can then be used to figure out the escape fraction of Lyman-Werner photons in the presence of shielding by H and H_2. Figure 9 shows this calculation of the escape fraction approximated by Schauer *et al.* (2015).

This treatment of Lyman-Werner radiation will be complemented by a prescription for calculating the stellar luminosity that will be used to estimate the fraction of photons in the Lyman-Werner bands. In the absence of observations of surviving first stars, we plan to approximate the stellar luminosity of the protostars in our simulations by assuming that they follow the Hayashi and Henyey tracks (Stacy *et al.*, 2016) as they evolve to reach the pre-main sequence phase

$$L_\star = L_{\rm acc} + L_{\rm int}\,, \tag{2.4}$$

by using a higher effective temperature than that suggested by these tracks (to find $L_{\rm int}$) because the gas is metal-free (Stahler *et al.*, 1986; Cassisi and Castellani, 1993). The accretion luminosity can be estimated as $L_{\rm acc} = GM_*\dot{M}/R_\star$ (Hartmann, 2008), where $\dot{M}$ is the accretion rate of the sink particle.

Another source of radiation feedback which is primarily important for the Pop III.2 star formation is cosmic rays driven by the Pop III.1 stars. It has been shown that the cosmic ray strength, even when varied for orders of magnitude, does not affect the evolution of a primordial cloud (Hummel *et al.*, 2015, 2016). However, these studies were carried out at lower resolutions where the small-scale turbulent magnetic fields could not be resolved and amplified, which are the necessary drivers for cosmic ray diffusion (Gabici *et al.*, 2007). We plan to include cosmic rays in the chemistry module by just treating the cosmic ray ionisation rate as a constant independent of position and time.

We note that we do not intend to perform 3D radiative transfer calculations. Apart from the computational costs involved, the reason for this is two-fold: 1.) the optically thick cooling rate which is defined as a fraction of the optically thin cooling rate in the KROME package has been shown to be a good approximation at densities of the order of $10^{15}\,\mathrm{cm}^{-3}$, which will be reached at the highest level of refinement in our simulations, and 2.) in the case

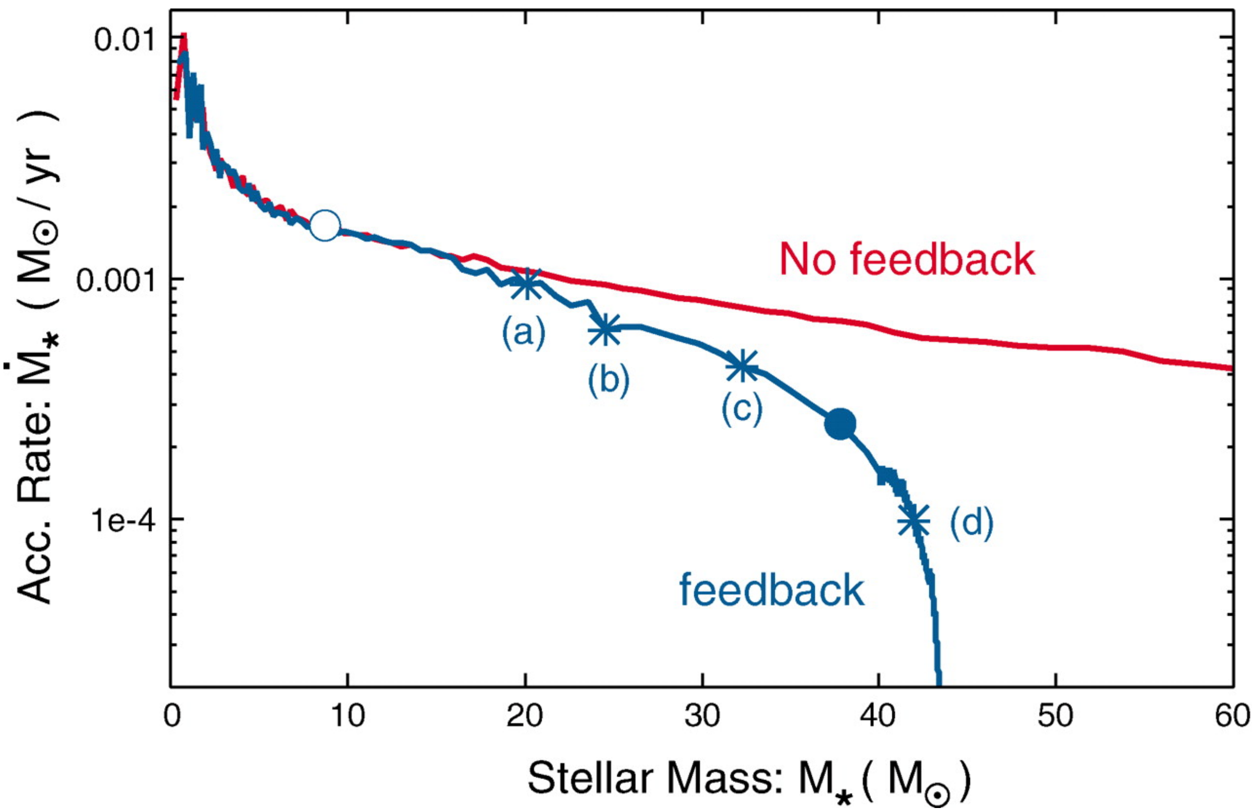

Figure 8: Figure adopted from Hosokawa *et al.* (2011), showing the accretion rate of a first star with and without the presence of radiation feedback. Radiation feedback from the protostar can halt its growth by evaporating the accretion disk around it (EUV radiation).

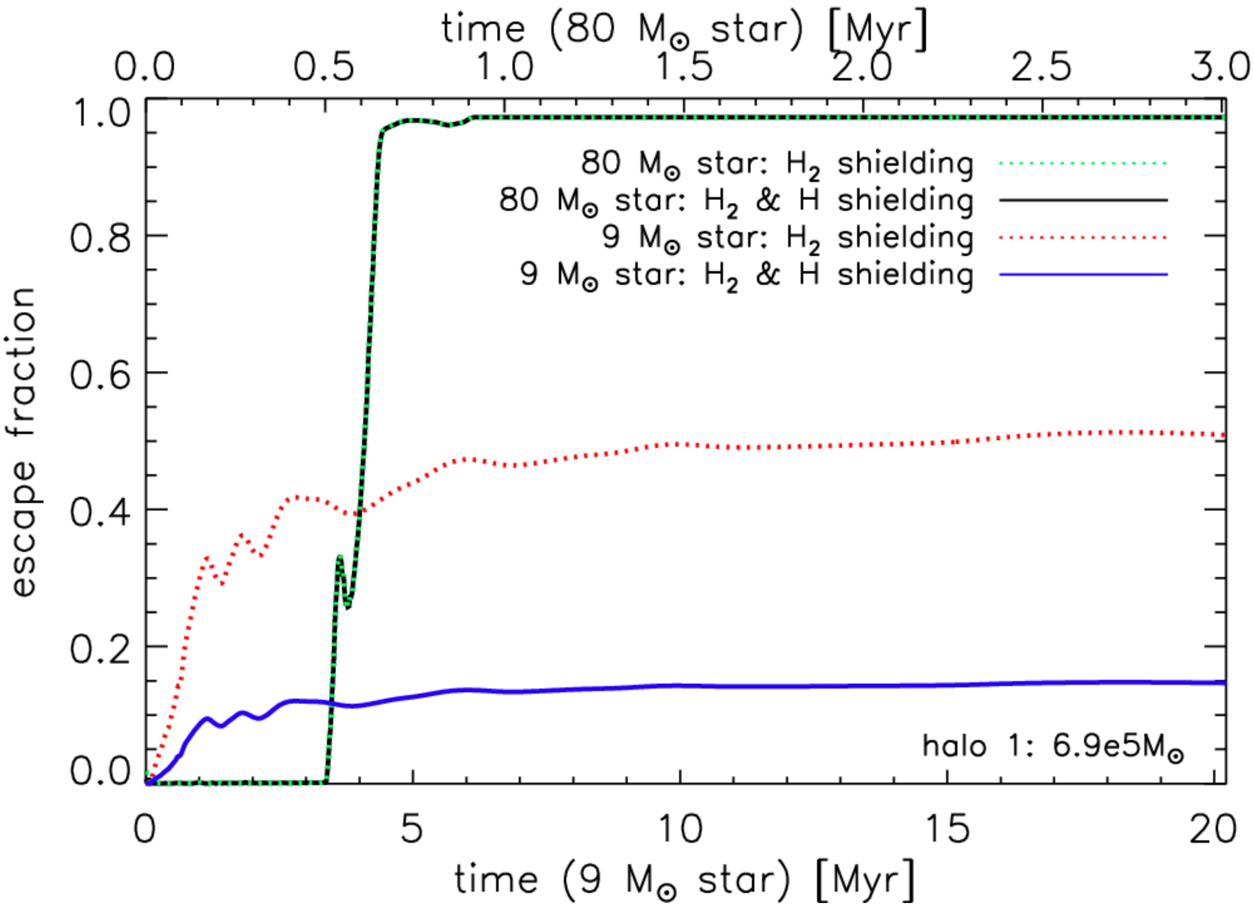

Figure 9: Figure adopted from Schauer *et al.* (2015), showing the escape fraction of Lyman-Werner photons for a massive and intermediate-mass star when shielding from H and H_2 is considered.

of primordial gas, cooling takes place due to line emissions instead of continuum emission as for present day star formation. It is harder to model radiative transfer in the former case because the medium is not static and the lines overlap in high density regions, thus deviating significantly from Lorentzian profiles.

In summary, the key additions from this research to the field of evolution of first stars can be:

1. Escape Fraction in the early Universe in the presence of turbulence
2. Restricted accretion and fragmentation in primordial gas in the presence of Lyman-Werner radiation.
3. The effects of Lyman-Werner radiation feedback on the mass distribution of the first stars.

3.0 SIDE PROJECTS

Apart from my primary focus on formation of the first stars, I plan to simultaneously work on two side projects. These projects deal with understanding star formation characteristics of high-redshift galaxies, and supernova feedback on star-forming molecular clouds. Hence, they are connected with the general field of star formation and can prove useful in the future to study the first galaxies and the first supernovae, respectively, as an extension of the PhD. They also provide me with experience on the observational front of studying the interstellar medium (ISM).

3.1 STAR FORMATION RATES IN SPATIALLY-RESOLVED HIGH-REDSHIFT GALAXIES

With: E. da Cunha, C. Federrath, A. M. Swinbank, S. Dye, E. Wisnioski, E. di Teodoro, K. Tadaki, M. S. Yun, I. Aretxaga, R. Kawabe

Numerous star formation relations have been proposed in a quest to universalize the theory of star formation, by linking the star formation rate (SFR) with the mass of gas, its freefall time, virial parameter, magnetic field strength and turbulence (Kennicutt 1998; Elmegreen 2002; Krumholz *et al.* 2012a; Federrath and Klessen 2012). While these relations have been shown to be valid for star-forming regions in the Milky Way and local galaxies (Bigiel *et al.*, 2008; Federrath *et al.*, 2016), the lack of spatial resolution has limited us in testing them on high-redshift sources with $z > 1$.

With the high-resolution data now available from ALMA, I plan to measure the star formation rates and gas properties in different regions of high-redshift starbursts using submm continuum and molecular line observations. The pipeline for this analysis has already been developed by Federrath *et al.* (2016) and Sharda *et al.* (2018). It requires fitting of modified-blackbody function to the galaxy's spectral energy distribution and integrating it to find the star formation rate. By comparing the measured rate with that predicted by semi-analytical models of star formation (Kennicutt, 1998; Krumholz *et al.*, 2012a; Salim *et al.*, 2015), I plan to find whether these models which have been well calibrated for local star-forming regions can also explain the star formation rate at high-redshifts (Sharda *et al.*, 2018; Sharda *et al.*, 2019). This can also help discover how high-redshift starbursts sustain high star formation rates and are often as metal-enriched as the Milky Way (Tadaki *et al.*, 2019).

3.2 X-RAY AND RADIO OBSERVATIONS OF THE SNR N132D IN THE LMC

With: P. Plucinsky, T. Gaetz, V. Kashyap, K. Jameson, N. Pingel, C. Federrath, B. Burkhart, M. Krumholz, N. Maxted, D. Milisavljevic, W. Blair, H. Sano, M. Sasaki and other members of the *Chandra*/ALMA Proposals

Supernova Remnant (SNR) N132D is the brightest SNR present in the LMC at multiple wavelengths of the electromagnetic spectrum (Dickel and Milne, 1995; Blair *et al.*, 2000; Borkowski *et al.*, 2007; H.E.S.S. Collaboration *et al.*, 2015). Based on optical observations, it has been classified as an Oxygen-rich SNR (Danziger and Dennefeld, 1976) which perhaps exploded inside a low-density cavity created by the winds of its progenitor (Sutherland and Dopita, 1995). This SNR is believed to be in the transition stage from young- to middle-aged remnants (Bamba *et al.*, 2018), making it a unique low-metallicity laboratory to probe supernova evolution and effects of an SNR on nearby star-forming and quiescent molecular clouds at high resolution.

Using archival *Chandra* data of the remnant, we have characterized the blast wave to find the local LMC average abundances of O, Ne, Mg, Si, S and Fe (Sharda et al., 2019b, in prep.). We have also detected signatures of recombining plasma in the remnant (see also, Hitomi Collaboration *et al.* 2018), which is crucial to understand the explosion of the progenitor. With the upcoming legacy *Chandra* observations of this remnant on which I am a Co-Investigator, I plan to work on the largest spatially-resolved X-ray dataset of a middle-aged remnant to produce the map of recombining plasma and accurately constrain the yields of S and Fe produced by the explosion. Further, if my ALMA Cycle 7 proposal to observe this remnant and the surrounding clouds through molecular line emissions at high resolution (0.4 pc) is accepted, I plan to use the ALMA data to study the modes of turbulence caused by SN shocks in molecular clouds and the acceleration of cosmic rays generated by N132D.

4.0 TIMELINE

1. 2018 Semester 2
   a. Setup FLASH ✓
   b. Setup KROME ✓
   c. Literature Review on First Stars ✓
   d. Work on SP1: Resolved Star Formation at High-Redshift ✓
   e. Course: Astrophysical Gas Dynamics ✓
2. 2019 Semester 1
   a. Setup Initial Conditions for Simulations ✓
   b. Include Primordial Chemistry in Simulations ✓
   c. Attend ANITA 2019 in Melbourne ✓
   d. Work on SP2: ALMA Proposal to Observe SNR N132D in the LMC (PI) ✓
   e. Publish Work on SP1 ✓(Sharda *et al.*, 2019)
3. 2019 Semester 2
   a. Work on the Thermodynamics of H_2 in Primordial Environments ✓
   b. Include Magnetic Fields in Simulations
   c. Work on Disk Fragmentation in the Presence of Magnetic Fields
   d. Work on SP2: *Chandra* X-ray data of SNR N132D (Co-I)
   e. Attend Star Formation Workshop at ISSI, Bern, Switzerland ✓
   f. Attend Summer School on First Stars at Sao Paulo in Brazil
4. 2020 Semester 1
   a. Publish Work on the Thermodynamics of H_2 in Primordial Environments
   b. Study Cosmological Simulations of the Early Universe
   c. Include Realistic Cosmological Initial Conditions in the Simulations

    d. Work on Accretion Characteristics of First Stars
    e. Publish Work on Effects of Turbulence and Magnetic Fields on the Formation of First Stars
    f. Attend First Stars VI Conference at University of Concepcion, Chile

5. 2020 Semester 2
    a. Extract Mini-Halos from Cosmological Simulations
    b. Work on Escape Fractions in the Presence of Turbulence
    c. Work on Lyman-Werner Radiation Feedback in First Stars
    d. Work on Radiative Transfer Module in FLASH
6. 2021 Semester 1
    a. Attend the IAU-GA in Korea
    b. Work on IMF of the First Stars
    c. Publish work on Radiation Feedback in Primordial Star Formation
    d. Attend Conference on Star Formation/Early Universe
7. 2021 Semester 2
    a. Publish Work on Convergence Towards IMF of First Stars
    b. Write Thesis
    c. Give End of Thesis Colloquium
    d. Submit Thesis

5.0 BIBLIOGRAPHY

T. Abel, P. Anninos, Y. Zhang, and M. L. Norman. Modeling primordial gas in numerical cosmology. *New Astronomy*, 2:181–207, August 1997.

T. Abel, G. L. Bryan, and M. L. Norman. The Formation of the First Star in the Universe. *Science*, 295:93–98, January 2002.

S. M. V. Aldrovandi and D. Pequignot. Ionization and Heating of a Low Density Plasma by Energetic Particles. *Astronomy and Astrophysics*, 26:33, July 1973.

A. C. Allison and A. Dalgarno. Photodissociation of Vibrationally Excited H_2, HD, and D_2 by Absorption into the Continua of the Lyman and Werner Systems. *Atomic Data*, 1:91, 1969.

A. Bamba, Y. Ohira, R. Yamazaki, M. Sawada, Y. Terada, K. Koyama, E. D. Miller, H. Yamaguchi, S. Katsuda, M. Nobukawa, and K. K. Nobukawa. The Transition from Young to Middle-aged Supernova Remnants: Thermal and Nonthermal Aspects of SNR N132D. *Astrophysical Journal*, 854:71, February 2018.

Robi Banerjee and Ralph E. Pudritz. Outflows and Jets from Collapsing Magnetized Cloud Cores. *Astrophysical Journal*, 641(2):949–960, Apr 2006.

M. R. Bate, I. A. Bonnell, and N. M. Price. Modelling accretion in protobinary systems. *Monthly Notices of the Royal Astronomical Society*, 277:362–376, November 1995.

M. R. Bate. Collapse of a Molecular Cloud Core to Stellar Densities: The First Three-dimensional Calculations. *Astrophysical Journal, Letters*, 508:L95–L98, November 1998.

F. Becerra, T. H. Greif, V. Springel, and L. E. Hernquist. Formation of massive protostars in atomic cooling haloes. *Monthly Notices of the Royal Astronomical Society*, 446:2380–2393, January 2015.

M. J. Berger and P. Colella. Local adaptive mesh refinement for shock hydrodynamics. *Journal of Computational Physics*, 82:64–84, May 1989.

F. Bigiel, A. Leroy, F. Walter, E. Brinks, W. J. G. de Blok, B. Madore, and M. D. Thornley. The Star Formation Law in Nearby Galaxies on Sub-Kpc Scales. *Astronomical Journal*, 136:2846–2871, December 2008.

D. C. Black and P. Bodenheimer. Evolution of rotating interstellar clouds. I - Numerical techniques. *Astrophysical Journal*, 199:619–632, August 1975.

W. P. Blair, J. A. Morse, J. C. Raymond, R. P. Kirshner, J. P. Hughes, M. A. Dopita, R. S. Sutherland, K. S. Long, and P. F. Winkler. Hubble Space Telescope Observations of Oxygen-rich Supernova Remnants in the Magellanic Clouds. II. Elemental Abundances in N132D and 1E 0102.2-7219. *Astrophysical Journal*, 537:667–689, July 2000.

A. Bleuler and R. Teyssier. Towards a more realistic sink particle algorithm for the RAMSES CODE. *Monthly Notices of the Royal Astronomical Society*, 445:4015–4036, December 2014.

A. C. Boley, T. W. Hartquist, R. H. Durisen, and S. Michael. The Internal Energy for Molecular Hydrogen in Gravitationally Unstable Protoplanetary Disks. *Astrophysical Journal, Letters*, 656:L89–L92, February 2007.

H. E. Bond. Where is Population III. *Astrophysical Journal*, 248:606–611, September 1981.

K. J. Borkowski, S. P. Hendrick, and S. P. Reynolds. X-Ray-Emitting Ejecta of Supernova Remnant N132D. *Astrophysical Journal, Letters*, 671:L45–L48, December 2007.

François Bouchut, Christian Klingenberg, and Knut Waagan. A multiwave approximate riemann solver for ideal mhd based on relaxation. i: theoretical framework. *Numerische Mathematik*, 108(1):7–42, Nov 2007.

François Bouchut, Christian Klingenberg, and Knut Waagan. A multiwave approximate riemann solver for ideal mhd based on relaxation ii: numerical implementation with 3 and 5 waves. *Numerische Mathematik*, 115(4):647–679, Jun 2010.

S. Bovino, T. Grassi, M. A. Latif, and D. R. G. Schleicher. Impact of an accurate modelling of primordial chemistry in high-resolution studies. *Monthly Notices of the Royal Astronomical Society*, 434:L36–L40, July 2013.

A. Brandenburg and K. Subramanian. Astrophysical magnetic fields and nonlinear dynamo theory. , 417:1–209, October 2005.

A. Brandenburg, D. Sokoloff, and K. Subramanian. Current Status of Turbulent Dynamo Theory. From Large-Scale to Small-Scale Dynamos. *Space Science Reviews*, 169:123–157, September 2012.

V. Bromm and R. B. Larson. The First Stars. *Annual Review of Astronomy and Astrophysics*, 42:79–118, September 2004.

V. Bromm, P. S. Coppi, and R. B. Larson. The Formation of the First Stars. I. The Primordial Star-forming Cloud. *Astrophysical Journal*, 564:23–51, January 2002.

L. Buntemeyer, R. Banerjee, T. Peters, M. Klassen, and R. E. Pudritz. Radiation hydrodynamics using characteristics on adaptive decomposed domains for massively parallel star formation simulations. *New Astronomy*, 43:49–69, February 2016.

Andreas Burkert and Peter Bodenheimer. Turbulent Molecular Cloud Cores: Rotational Properties. *Astrophysical Journal*, 543(2):822–830, Nov 2000.

M. Capitelli, C. M. Coppola, P. Diomede, and S. Longo. An evaluation of the effect of the dissociative attachment of vibrationally excited H{2} on primordial universe chemistry. *Astronomy and Astrophysics*, 470:811–813, August 2007.

A. R. Casey and K. C. Schlaufman. Chemistry of the Most Metal-poor Stars in the Bulge and the z 10 Universe. *Astrophysical Journal*, 809:110, August 2015.

S. Cassisi and V. Castellani. An evolutionary scenario for primeval stellar populations. *Astrophysical Journal, Supplement*, 88:509–527, October 1993.

R. Cen. A hydrodynamic approach to cosmology - Methodology. *Astrophysical Journal, Supplement*, 78:341–364, February 1992.

V. Cheera and R. Nigam. Effects of primordial magnetic field on the formation rate of dark matter halos. *Astrophysics and Space Science*, 363:93, May 2018.

B. Ciardi and A. Ferrara. The First Cosmic Structures and Their Effects. *Space Science Reviews*, 116:625–705, February 2005.

P. C. Clark, S. C. O. Glover, R. J. Smith, T. H. Greif, R. S. Klessen, and V. Bromm. The Formation and Fragmentation of Disks Around Primordial Protostars. *Science*, 331:1040, February 2011.

Paul C. Clark, Simon C. O. Glover, Ralf S. Klessen, and Volker Bromm. Gravitational Fragmentation in Turbulent Primordial Gas and the Initial Mass Function of Population III Stars. *Astrophysical Journal*, 727(2):110, Feb 2011.

C. M. Coppola, L. Lodi, and J. Tennyson. Radiative cooling functions for primordial molecules. *Monthly Notices of the Royal Astronomical Society*, 415:487–493, July 2011.

Richard M. Crutcher. Magnetic Fields in Molecular Clouds: Observations Confront Theory. *Astrophysical Journal*, 520(2):706–713, Aug 1999.

A. Dalgarno and S. Lepp. Chemistry in the early universe. In M. S. Vardya and S. P. Tarafdar, editors, *Astrochemistry*, volume 120 of *IAU Symposium*, pages 109–118, 1987.

I. J. Danziger and M. Dennefeld. Supernova ejecta in the Large Magellanic Cloud. *Astrophysical Journal*, 207:394–407, July 1976.

R. S. de Souza, N. Yoshida, and K. Ioka. Populations III.1 and III.2 gamma-ray bursts: constraints on the event rate for future radio and X-ray surveys. *Astronomy and Astrophysics*, 533:A32, Sep 2011.

J. R. Dickel and D. K. Milne. Radio properties of three young supernova remnants in the Large Magellanic Cloud. *Astronomical Journal*, 109:200–208, January 1995.

B. T. Draine and F. Bertoldi. Structure of Stationary Photodissociation Fronts. *Astrophysical Journal*, 468:269, September 1996.

M. Druschke, A. T. P. Schauer, S. C. O. Glover, and R. S. Klessen. Shape and spin of minihaloes: from large scales to the centres. *Monthly Notices of the Royal Astronomical Society*, 481:3266–3277, December 2018.

A. Dubey, R. Fisher, C. Graziani, G. C. Jordan, IV, D. Q. Lamb, L. B. Reid, P. Rich, D. Sheeler, D. Townsley, and K. Weide. Challenges of Extreme Computing using the FLASH code. In N. V. Pogorelov, E. Audit, and G. P. Zank, editors, *Numerical Modeling of Space Plasma Flows*, volume 385 of *Astronomical Society of the Pacific Conference Series*, page 145, April 2008.

B. G. Elmegreen. Star Formation from Galaxies to Globules. *Astrophysical Journal*, 577:206–220, September 2002.

X. Fan. Evolution of high-redshift quasars. *New Astronomy Review*, 50:665–671, November 2006.

C. Federrath and R. S. Klessen. The Star Formation Rate of Turbulent Magnetized Clouds: Comparing Theory, Simulations, and Observations. *Astrophysical Journal*, 761:156, December 2012.

Christoph Federrath, Robi Banerjee, Paul C. Clark, and Ralf S. Klessen. Modeling Collapse and Accretion in Turbulent Gas Clouds: Implementation and Comparison of Sink Particles in AMR and SPH. *Astrophysical Journal*, 713:269–290, April 2010.

C. Federrath, S. Sur, D. R. G. Schleicher, R. Banerjee, and R. S. Klessen. A New Jeans Resolution Criterion for (M)HD Simulations of Self-gravitating Gas: Application to Magnetic Field Amplification by Gravity-driven Turbulence. *Astrophysical Journal*, 731:62, April 2011.

C. Federrath, J. Schober, S. Bovino, and D. R. G. Schleicher. The Turbulent Dynamo in Highly Compressible Supersonic Plasmas. *Astrophysical Journal, Letters*, 797:L19, December 2014.

C. Federrath, J. M. Rathborne, S. N. Longmore, J. M. D. Kruijssen, J. Bally, Y. Contreras, R. M. Crocker, G. Garay, J. M. Jackson, L. Testi, and A. J. Walsh. The Link between Turbulence, Magnetic Fields, Filaments, and Star Formation in the Central Molecular Zone Cloud G0.253+0.016. *Astrophysical Journal*, 832:143, December 2016.

A. Fialkov, R. Barkana, and E. Visbal. The observable signature of late heating of the Universe during cosmic reionization. , 506:197–199, February 2014.

Brian D. Fields. The Primordial Lithium Problem. *Annual Review of Nuclear and Particle Science*, 61(1):47–68, Nov 2011.

R. C. Forrey. Rate of Formation of Hydrogen Molecules by Three-body Recombination during Primordial Star Formation. *Astrophysical Journal, Letters*, 773:L25, August 2013.

A. Frebel and J. E. Norris. Near-Field Cosmology with Extremely Metal-Poor Stars. *Annual Review of Astronomy and Astrophysics*, 53:631–688, August 2015.

B. Fryxell, K. Olson, P. Ricker, F. X. Timmes, M. Zingale, D. Q. Lamb, P. MacNeice, R. Rosner, J. W. Truran, and H. Tufo. FLASH: An Adaptive Mesh Hydrodynamics Code for Modeling Astrophysical Thermonuclear Flashes. *Astrophysical Journal, Supplement*, 131:273–334, November 2000.

S. Gabici, F. A. Aharonian, and P. Blasi. Gamma rays from molecular clouds. *Astrophysics and Space Science*, 309:365–371, June 2007.

D. Galli and F. Palla. The chemistry of the early Universe. *Astronomy and Astrophysics*, 335:403–420, July 1998.

D. Galli and F. Palla. Deuterium chemistry in the primordial gas. , 50:1197–1204, October 2002.

D. Galli and F. Palla. The Dawn of Chemistry. *Annual Review of Astronomy and Astrophysics*, 51:163–206, August 2013.

L. Gao, N. Yoshida, T. Abel, C. S. Frenk, A. Jenkins, and V. Springel. The first generation of stars in the Λ cold dark matter cosmology. *Monthly Notices of the Royal Astronomical Society*, 378:449–468, June 2007.

I. A. Gerrard, C. Federrath, and R. Kuruwita. The role of initial magnetic field structure in the launching of protostellar jets. *Monthly Notices of the Royal Astronomical Society*, 485:5532–5542, June 2019.

Carl H. Gibson. Dark Matter as Fossil Turbulence—Primordial Fog Particles and WIMPs. In *APS Division of Fluid Dynamics Meeting Abstracts*, page AD.09, Nov 1996.

S. C. O. Glover and T. Abel. Uncertainties in H_2 and HD chemistry and cooling and their role in early structure formation. *Monthly Notices of the Royal Astronomical Society*, 388:1627–1651, August 2008.

S. C. O. Glover and A.-K. Jappsen. Star Formation at Very Low Metallicity. I. Chemistry and Cooling at Low Densities. *Astrophysical Journal*, 666:1–19, September 2007.

S. C. O. Glover and D. W. Savin. Is H_3^+ cooling ever important in primordial gas? *Monthly Notices of the Royal Astronomical Society*, 393:911–948, March 2009.

S. C. O. Glover, C. Federrath, M.-M. Mac Low, and R. S. Klessen. Simulating the chemistry and dynamics of molecular clouds. *Highlights of Astronomy*, 15:405–405, November 2010.

S. Glover. The Formation Of The First Stars In The Universe. *Space Science Reviews*, 117:445–508, April 2005.

H. Gong and E. C. Ostriker. Implementation of Sink Particles in the Athena Code. *Astrophysical Journal, Supplement*, 204:8, January 2013.

T. Grassi, S. Bovino, D. Schleicher, and F. A. Gianturco. Chemical complexity in astrophysical simulations: optimization and reduction techniques. *Monthly Notices of the Royal Astronomical Society*, 431:1659–1668, May 2013.

T. Grassi, S. Bovino, D. R. G. Schleicher, J. Prieto, D. Seifried, E. Simoncini, and F. A. Gianturco. KROME - a package to embed chemistry in astrophysical simulations. *Monthly Notices of the Royal Astronomical Society*, 439:2386–2419, April 2014.

Thomas H. Greif, Jarrett L. Johnson, Ralf S. Klessen, and Volker Bromm. The first galaxies: assembly, cooling and the onset of turbulence. *Monthly Notices of the Royal Astronomical Society*, 387(3):1021–1036, Jul 2008.

T. H. Greif, V. Springel, S. D. M. White, S. C. O. Glover, P. C. Clark, R. J. Smith, R. S. Klessen, and V. Bromm. Simulations on a Moving Mesh: The Clustered Formation of Population III Protostars. *Astrophysical Journal*, 737:75, August 2011.

T. H. Greif, V. Bromm, P. C. Clark, S. C. O. Glover, R. J. Smith, R. S. Klessen, N. Yoshida, and V. Springel. Formation and evolution of primordial protostellar systems. *Monthly Notices of the Royal Astronomical Society*, 424:399–415, July 2012.

B. F. Griffen, G. A. Dooley, A. P. Ji, B. W. O'Shea, F. A. Gómez, and A. Frebel. Tracing the first stars and galaxies of the Milky Way. *Monthly Notices of the Royal Astronomical Society*, 474:443–459, February 2018.

D. Guszejnov, P. F. Hopkins, M. Y. Grudić, M. R. Krumholz, and C. Federrath. Isothermal Fragmentation: Is there a low-mass cut-off? *Monthly Notices of the Royal Astronomical Society*, 480:182–191, October 2018.

L. Hartmann. *Accretion Processes in Star Formation.* November 2008.

T. Hartwig, M. N. Ishigaki, R. S. Klessen, and N. Yoshida. Fingerprint of the first stars: multi-enriched extremely metal-poor stars in the TOPoS survey. *Monthly Notices of the Royal Astronomical Society*, 482:1204–1210, January 2019.

N. E. Haugen, A. Brandenburg, and W. Dobler. Simulations of nonhelical hydromagnetic turbulence. , 70(1):016308, July 2004.

H.E.S.S. Collaboration, A. Abramowski, F. Aharonian, F. Ait Benkhali, A. G. Akhperjanian, E. O. Angüner, M. Backes, S. Balenderan, A. Balzer, A. Barnacka, and et al. The exceptionally powerful TeV γ-ray emitters in the Large Magellanic Cloud. *Science*, 347:406–412, January 2015.

S. Hirano and V. Bromm. Formation and survival of Population III stellar systems. *Monthly Notices of the Royal Astronomical Society*, 470:898–914, September 2017.

S. Hirano and N. Yoshida. Radiative Cooling Implementations in Simulations of Primordial Star Formation. *Astrophysical Journal*, 763:52, January 2013.

S. Hirano, T. Hosokawa, N. Yoshida, H. Umeda, K. Omukai, G. Chiaki, and H. W. Yorke. One Hundred First Stars: Protostellar Evolution and the Final Masses. *Astrophysical Journal*, 781:60, February 2014.

S. Hirano, T. Hosokawa, N. Yoshida, K. Omukai, and H. W. Yorke. Primordial star formation under the influence of far ultraviolet radiation: 1540 cosmological haloes and the stellar mass distribution. *Monthly Notices of the Royal Astronomical Society*, 448:568–587, March 2015.

S. Hirano, N. Yoshida, Y. Sakurai, and M. S. Fujii. Formation of the First Star Clusters and Massive Star Binaries by Fragmentation of Filamentary Primordial Gas Clouds. *Astrophysical Journal*, 855:17, March 2018.

Hitomi Collaboration, F. Aharonian, H. Akamatsu, F. Akimoto, S. W. Allen, L. Angelini, M. Audard, H. Awaki, M. Axelsson, A. Bamba, M. W. Bautz, R. Blandford, L. W. Brenneman, G. V. Brown, E. Bulbul, E. M. Cackett, M. Chernyakova, M. P. Chiao, P. S. Coppi, E. Costantini, J. de Plaa, C. P. de Vries, J.-W. den Herder, C. Done, T. Dotani, K. Ebisawa, M. E. Eckart, T. Enoto, Y. Ezoe, A. C. Fabian, C. Ferrigno, A. R. Foster, R. Fujimoto, Y. Fukazawa, A. Furuzawa, M. Galeazzi, L. C. Gallo, P. Gandhi, M. Giustini, A. Goldwurm, L. Gu, M. Guainazzi, Y. Haba, K. Hagino, K. Hamaguchi, I. M. Harrus, I. Hatsukade, K. Hayashi, T. Hayashi, K. Hayashida, J. S. Hiraga, A. Hornschemeier, A. Hoshino, J. P. Hughes, Y. Ichinohe, R. Iizuka, H. Inoue, Y. Inoue, M. Ishida, K. Ishikawa, Y. Ishisaki, M. Iwai, J. Kaastra, T. Kallman, T. Kamae, J. Kataoka, S. Katsuda, N. Kawai, R. L. Kelley, C. A. Kilbourne, T. Kitaguchi, S. Kitamoto, T. Kitayama, T. Kohmura, M. Kokubun, K. Koyama, S. Koyama, P. Kretschmar, H. A. Krimm, A. Kubota, H. Kunieda, P. Laurent, S.-H. Lee, M. A. Leutenegger, O. Limousin, M. Loewenstein, K. S. Long, D. Lumb, G. Madejski, Y. Maeda, D. Maier, K. Makishima, M. Markevitch, H. Matsumoto, K. Matsushita, D. McCammon, B. R. McNamara, M. Mehdipour, E. D. Miller, J. M. Miller, S. Mineshige, K. Mitsuda, I. Mitsuishi, T. Miyazawa, T. Mizuno, H. Mori, K. Mori, K. Mukai, H. Murakami, R. F. Mushotzky, T. Nakagawa, H. Nakajima, T. Nakamori, S. Nakashima, K. Nakazawa, K. K. Nobukawa, M. Nobukawa, H. Noda, H. Odaka, T. Ohashi, M. Ohno, T. Okajima, N. Ota, M. Ozaki, F. Paerels, S. Paltani, R. Petre, C. Pinto, F. S. Porter, K. Pottschmidt, C. S. Reynolds, S. Safi-Harb, S. Saito, K. Sakai, T. Sasaki, G. Sato, K. Sato, R. Sato, T. Sato, M. Sawada, N. Schartel, P. J. Serlemtsos, H. Seta, M. Shidatsu, A. Simionescu, R. K. Smith, Y. Soong, Ł. Stawarz, Y. Sugawara, S. Sugita, A. Szymkowiak, H. Tajima, H. Takahashi, T. Takahashi, S. Takeda, Y. Takei, T. Tamagawa, T. Tamura, T. Tanaka, Y. Tanaka, Y. T. Tanaka, M. S. Tashiro, Y. Tawara, Y. Terada, Y. Terashima, F. Tombesi, H. Tomida, Y. Tsuboi, M. Tsujimoto, H. Tsunemi, T. G. Tsuru, H. Uchida, H. Uchiyama, Y. Uchiyama, S. Ueda, Y. Ueda, S. Uno, C. M. Urry, E. Ursino, S. Watanabe, N. Werner, D. R. Wilkins, B. J. Williams, S. Yamada, H. Yamaguchi, K. Yamaoka, N. Y. Yamasaki, M. Yamauchi, S. Yamauchi, T. Yaqoob, Y. Yatsu, D. Yonetoku, I. Zhuravleva, and A. Zoghbi. Hitomi observations of the LMC SNR N 132 D: Highly redshifted X-ray emission from iron ejecta. *Publications of the ASJ*, 70:16, March 2018.

T. Hosokawa, K. Omukai, N. Yoshida, and H. W. Yorke. Protostellar Feedback Halts the Growth of the First Stars in the Universe. *Science*, 334:1250, December 2011.

T. Hosokawa, S. Hirano, R. Kuiper, H. W. Yorke, K. Omukai, and N. Yoshida. Formation of Massive Primordial Stars: Intermittent UV Feedback with Episodic Mass Accretion. *Astrophysical Journal*, 824:119, June 2016.

L. M. Howes, A. R. Casey, M. Asplund, S. C. Keller, D. Yong, D. M. Nataf, R. Poleski, K. Lind, C. Kobayashi, C. I. Owen, M. Ness, M. S. Bessell, G. S. da Costa, B. P. Schmidt, P. Tisserand, A. Udalski, M. K. Szymański, I. Soszyński, G. Pietrzyński, K. Ulaczyk, Ł. Wyrzykowski, P. Pietrukowicz, J. Skowron, S. Kozłowski, and P. Mróz. Extremely metal-poor stars from the cosmic dawn in the bulge of the Milky Way. , 527:484–487, November 2015.

D. A. Hubber, S. A. E. G. Falle, and S. P. Goodwin. Convergence of AMR and SPH simulations - I. Hydrodynamical resolution and convergence tests. *Monthly Notices of the Royal Astronomical Society*, 432:711–727, June 2013.

D. A. Hubber, S. Walch, and A. P. Whitworth. An improved sink particle algorithm for SPH simulations. *Monthly Notices of the Royal Astronomical Society*, 430:3261–3275, April 2013.

J. A. Hummel, A. Stacy, M. Jeon, A. Oliveri, and V. Bromm. The first stars: formation under X-ray feedback. *Monthly Notices of the Royal Astronomical Society*, 453:4136–4147, November 2015.

J. A. Hummel, A. Stacy, and V. Bromm. The first stars: formation under cosmic ray feedback. *Monthly Notices of the Royal Astronomical Society*, 460:2432–2444, August 2016.

R. K. Janev, W. D. Langer, and K. Evans. *Elementary processes in Hydrogen-Helium plasmas - Cross sections and reaction rate coefficients*. 1987.

A.-K. Jappsen, R. S. Klessen, R. B. Larson, Y. Li, and M.-M. Mac Low. The stellar mass spectrum from non-isothermal gravoturbulent fragmentation. *Astronomy and Astrophysics*, 435:611–623, May 2005.

J. H. Jeans. The Stability of a Spherical Nebula. *Philosophical Transactions of the Royal Society of London Series A*, 199:1–53, 1902.

M. O. Jones and M. R. Bate. Sink particle radiative feedback in smoothed particle hydrodynamics models of star formation. *Monthly Notices of the Royal Astronomical Society*, 480:2562–2577, October 2018.

T. Kahniashvili, Y. Maravin, A. Natarajan, N. Battaglia, and A. G. Tevzadze. Constraining Primordial Magnetic Fields through Large-scale Structure. *Astrophysical Journal*, 770:47, June 2013.

T. Kahniashvili, Y. Maravin, G. Lavrelashvili, and A. Kosowsky. Primordial magnetic helicity constraints from WMAP nine-year data. , 90(8):083004, October 2014.

R. C. Kennicutt, Jr. Star Formation in Galaxies Along the Hubble Sequence. *Annual Review of Astronomy and Astrophysics*, 36:189–232, 1998.

S. Kitsionas, C. Federrath, R. S. Klessen, W. Schmidt, D. J. Price, L. J. Dursi, M. Gritschneder, S. Walch, R. Piontek, J. Kim, A.-K. Jappsen, P. Ciecielag, and M.-M. Mac Low. Algorithmic comparisons of decaying, isothermal, supersonic turbulence. *Astronomy and Astrophysics*, 508:541–560, December 2009.

Ralf S. Klessen. Formation of the first stars. *arXiv e-prints*, page arXiv:1807.06248, Jul 2018.

H. Kreckel, H. Bruhns, M. Čížek, S. C. O. Glover, K. A. Miller, X. Urbain, and D. W. Savin. Experimental Results for H_2 Formation from H^- and H and Implications for First Star Formation. *Science*, 329:69, July 2010.

M. R. Krumholz, C. F. McKee, and R. I. Klein. Embedding Lagrangian Sink Particles in Eulerian Grids. *Astrophysical Journal*, 611:399–412, August 2004.

M. R. Krumholz, A. Dekel, and C. F. McKee. A Universal, Local Star Formation Law in Galactic Clouds, nearby Galaxies, High-redshift Disks, and Starbursts. *Astrophysical Journal*, 745:69, January 2012.

Mark R. Krumholz, Richard I. Klein, and Christopher F. McKee. Radiation-hydrodynamic Simulations of the Formation of Orion-like Star Clusters. II. The Initial Mass Function from Winds, Turbulence, and Radiation. *Astrophysical Journal*, 754(1):71, Jul 2012.

M. R. Krumholz. DESPOTIC - a new software library to Derive the Energetics and SPectra of Optically Thick Interstellar Clouds. *Monthly Notices of the Royal Astronomical Society*, 437:1662–1680, January 2014.

R. B. Larson. Numerical calculations of the dynamics of collapsing proto-star. *Monthly Notices of the Royal Astronomical Society*, 145:271, 1969.

M. A. Latif and D. R. G. Schleicher. Magnetic fields in primordial accretion disks. *Astronomy and Astrophysics*, 585:A151, January 2016.

S. Lepp and J. M. Shull. Molecules in the early universe. *Astrophysical Journal*, 280:465–469, May 1984.

B. T. Lewis and M. R. Bate. Shaken and stirred: the effects of turbulence and rotation on disc and outflow formation during the collapse of magnetized molecular cloud cores. *Monthly Notices of the Royal Astronomical Society*, 477:4241–4256, July 2018.

M. N. Machida and K. Doi. The formation of Population III stars in gas accretion stage: effects of magnetic fields. *Monthly Notices of the Royal Astronomical Society*, 435:3283–3305, November 2013.

M. N. Machida, T. Matsumoto, and S.-i. Inutsuka. Magnetohydrodynamics of Population III Star Formation. *Astrophysical Journal*, 685:690–704, October 2008.

M. N. Machida, K. Omukai, T. Matsumoto, and S.-i. Inutsuka. Conditions for the Formation of First-Star Binaries. *Astrophysical Journal*, 677:813–827, April 2008.

U. Maio, S. Khochfar, J. L. Johnson, and B. Ciardi. The interplay between chemical and mechanical feedback from the first generation of stars. *Monthly Notices of the Royal Astronomical Society*, 414:1145–1157, June 2011.

H. Maki and H. Susa. Dissipation of Magnetic Flux in Primordial Gas Clouds. *Astrophysical Journal*, 609:467–473, July 2004.

F. Marinacci, M. Vogelsberger, R. Pakmor, P. Torrey, V. Springel, L. Hernquist, D. Nelson, R. Weinberger, A. Pillepich, J. Naiman, and S. Genel. First results from the IllustrisTNG simulations: radio haloes and magnetic fields. *Monthly Notices of the Royal Astronomical Society*, 480:5113–5139, November 2018.

S. L. Martell, S. Sharma, S. Buder, L. Duong, K. J. Schlesinger, J. Simpson, K. Lind, M. Ness, J. P. Marshall, M. Asplund, J. Bland-Hawthorn, A. R. Casey, G. De Silva, K. C. Freeman, J. Kos, J. Lin, D. B. Zucker, T. Zwitter, B. Anguiano, C. Bacigalupo, D. Carollo, L. Casagrande, G. S. Da Costa, J. Horner, D. Huber, E. A. Hyde, P. R. Kafle, G. F. Lewis, D. Nataf, C. A. Navin, D. Stello, C. G. Tinney, F. G. Watson, and R. Wittenmyer. The GALAH survey: observational overview and Gaia DR1 companion. *Monthly Notices of the Royal Astronomical Society*, 465:3203–3219, March 2017.

Manyalibo J. Matthews, Guillaume Petitpas, and Salvador M. Aceves. A study of spin isomer conversion kinetics in supercritical fluid hydrogen for cryogenic fuel storage technologies. *Applied Physics Letters*, 99(8):081906, 2011.

J. C. McDowell. The light from Population III stars. *Monthly Notices of the Royal Astronomical Society*, 223:763–786, December 1986.

C. F. McKee and J. C. Tan. The Formation of the First Stars. II. Radiative Feedback Processes and Implications for the Initial Mass Function. *Astrophysical Journal*, 681:771–797, July 2008.

G. F. Mitchell and T. J. Deveau. Effects of a shock on the molecular composition of a diffuse interstellar cloud. *Astrophysical Journal*, 266:646–661, March 1983.

P. A. Oesch, G. Brammer, P. G. van Dokkum, G. D. Illingworth, R. J. Bouwens, I. Labbé, M. Franx, I. Momcheva, M. L. N. Ashby, G. G. Fazio, V. Gonzalez, B. Holden, D. Magee, R. E. Skelton, R. Smit, L. R. Spitler, M. Trenti, and S. P. Willner. A Remarkably Luminous Galaxy at z=11.1 Measured with Hubble Space Telescope Grism Spectroscopy. *Astrophysical Journal*, 819(2):129, Mar 2016.

K. Omukai and R. Nishi. Formation of Primordial Protostars. *Astrophysical Journal*, 508:141–150, November 1998.

K. Omukai, T. Tsuribe, R. Schneider, and A. Ferrara. Thermal and Fragmentation Properties of Star-forming Clouds in Low-Metallicity Environments. *Astrophysical Journal*, 626:627–643, June 2005.

K. Omukai, R. Schneider, and Z. Haiman. Can Supermassive Black Holes Form in Metal-enriched High-Redshift Protogalaxies? *Astrophysical Journal*, 686:801–814, October 2008.

K. Omukai. Primordial Star Formation under Far-Ultraviolet Radiation. *Astrophysical Journal*, 546:635–651, January 2001.

B. W. O'Shea and M. L. Norman. Population III Star Formation in a ΛCDM Universe. I. The Effect of Formation Redshift and Environment on Protostellar Accretion Rate. *Astrophysical Journal*, 654:66–92, January 2007.

Brian W. O'Shea, Kentaro Nagamine, Volker Springel, Lars Hernquist, and Michael L. Norman. Comparing AMR and SPH Cosmological Simulations. I. Dark Matter and Adiabatic Simulations. *Astrophysical Journal, Supplement*, 160(1):1–27, Sep 2005.

Paolo Padoan and Åke Nordlund. The Star Formation Rate of Supersonic Magnetohydrodynamic Turbulence. *Astrophysical Journal*, 730(1):40, Mar 2011.

Vladimir I. Pariev and Stirling A. Colgate. A Magnetic α-ω Dynamo in AGN Disks. I. The Hydrodynamics of Star-Disk Collisions and Keplerian Flow. *Astrophysical Journal*, 658(1):114–128, Mar 2007.

Vladimir I. Pariev, Stirling A. Colgate, and J. M. Finn. A Magnetic α-ω Dynamo in AGN Disks. II. Magnetic Field Generation, Theories, and Simulations. *Astrophysical Journal*, 658(1):129–160, Mar 2007.

P. J. E. Peebles. Recombination of the Primeval Plasma. *Astrophysical Journal*, 153:1, July 1968.

Tomek Plewa. Numerical Hydrodynamics: SPH versus AMR. In H. Zinnecker and R. Mathieu, editors, *The Formation of Binary Stars*, volume 200 of *IAU Symposium*, page 563, Jan 2001.

Daniel J. Price and Matthew R. Bate. The impact of magnetic fields on single and binary star formation. *Monthly Notices of the Royal Astronomical Society*, 377(1):77–90, May 2007.

R. E. Pudritz and C. A. Norman. Bipolar Hydromagnetic Winds from Disks around Protostellar Objects. *Astrophysical Journal*, 301:571, Feb 1986.

J. A. Regan and T. P. Downes. Fragmentation inside atomic cooling haloes exposed to Lyman-Werner radiation. *Monthly Notices of the Royal Astronomical Society*, 475:4636–4647, April 2018.

E. Ripamonti and T. Abel. Fragmentation and the formation of primordial protostars: the possible role of collision-induced emission. *Monthly Notices of the Royal Astronomical Society*, 348:1019–1034, March 2004.

M. Rocha, A. H. G. Peter, J. S. Bullock, M. Kaplinghat, S. Garrison-Kimmel, J. Oñorbe, and L. A. Moustakas. Cosmological simulations with self-interacting dark matter - I. Constant-density cores and substructure. *Monthly Notices of the Royal Astronomical Society*, 430:81–104, March 2013.

M. Safarzadeh and E. Scannapieco. The Impact of Unresolved Turbulence on the Escape Fraction of Lyman Continuum Photons. *Astrophysical Journal*, 832(1):L9, Nov 2016.

S. Saga, H. Tashiro, and S. Yokoyama. Limits on primordial magnetic fields from direct detection experiments of gravitational wave background. , 98(8):083518, October 2018.

K. Saigo, T. Matsumoto, and M. Umemura. The Formation of Population III Binaries. *Astrophysical Journal, Letters*, 615:L65–L68, November 2004.

D. M. Salim, C. Federrath, and L. J. Kewley. A Universal, Turbulence-regulated Star Formation Law: From Milky Way Clouds to High-redshift Disk and Starburst Galaxies. *Astrophysical Journal, Letters*, 806:L36, June 2015.

D. W. Savin, P. S. Krstić, Z. Haiman, and P. C. Stancil. Rate Coefficient for $\mathrm{H}^+ + \mathrm{H}_2(\mathrm{X}^1\Sigma^+{}_g, \nu = 0, \mathrm{J} = 0) - \mathrm{H}(1s) + \mathrm{H}^+{}_2$ Charge Transfer and Some Cosmological Implications. *Astrophysical Journal, Letters*, 606:L167–L170, May 2004.

A. T. P. Schauer, D. J. Whalen, S. C. O. Glover, and R. S. Klessen. Lyman-Werner UV escape fractions from primordial haloes. *Monthly Notices of the Royal Astronomical Society*, 454:2441–2450, December 2015.

A. T. P. Schauer, B. Agarwal, S. C. O. Glover, R. S. Klessen, M. A. Latif, L. Mas-Ribas, C.-E. Rydberg, D. J. Whalen, and E. Zackrisson. Lyman-Werner escape fractions from the first galaxies. *Monthly Notices of the Royal Astronomical Society*, 467:2288–2300, May 2017.

J. Schaye, R. A. Crain, R. G. Bower, M. Furlong, M. Schaller, T. Theuns, C. Dalla Vecchia, C. S. Frenk, I. G. McCarthy, J. C. Helly, A. Jenkins, Y. M. Rosas-Guevara, S. D. M. White, M. Baes, C. M. Booth, P. Camps, J. F. Navarro, Y. Qu, A. Rahmati, T. Sawala, P. A. Thomas, and J. Trayford. The EAGLE project: simulating the evolution and assembly of galaxies and their environments. *Monthly Notices of the Royal Astronomical Society*, 446:521–554, January 2015.

J. Schober, D. Schleicher, C. Federrath, S. Glover, R. S. Klessen, and R. Banerjee. The Small-scale Dynamo and Non-ideal Magnetohydrodynamics in Primordial Star Formation. *Astrophysical Journal*, 754:99, August 2012.

J. Schober, D. R. G. Schleicher, C. Federrath, S. Bovino, and R. S. Klessen. Saturation of the turbulent dynamo. , 92(2):023010, Aug 2015.

P. Sharda, C. Federrath, E. da Cunha, A. M. Swinbank, and S. Dye. Testing star formation laws in a starburst galaxy at redshift 3 resolved with ALMA. *Monthly Notices of the Royal Astronomical Society*, 477:4380–4390, July 2018.

P Sharda, E da Cunha, C Federrath, E Wisnioski, E M Di Teodoro, K Tadaki, M S Yun, I Aretxaga, and R Kawabe. Testing Star Formation Laws on Spatially Resolved Regions in a z âĽĹ 4.3 Starburst Galaxy. *Monthly Notices of the Royal Astronomical Society*, 06 2019.

J. D. Silverman, P. J. Green, W. A. Barkhouse, D.-W. Kim, M. Kim, B. J. Wilkes, R. A. Cameron, G. Hasinger, B. T. Jannuzi, M. G. Smith, P. S. Smith, and H. Tananbaum. The Luminosity Function of X-Ray-selected Active Galactic Nuclei: Evolution of Supermassive Black Holes at High Redshift. *Astrophysical Journal*, 679:118–139, May 2008.

R. J. Smith, T. Hosokawa, K. Omukai, S. C. O. Glover, and R. S. Klessen. Variable accretion rates and fluffy first stars. *Monthly Notices of the Royal Astronomical Society*, 424:457–463, July 2012.

D. Sobral, J. Matthee, B. Darvish, D. Schaerer, B. Mobasher, H. J. A. Röttgering, S. Santos, and S. Hemmati. Evidence for PopIII-like Stellar Populations in the Most Luminous Lyman-α Emitters at the Epoch of Reionization: Spectroscopic Confirmation. *Astrophysical Journal*, 808:139, August 2015.

Volker Springel. The cosmological simulation code GADGET-2. *Monthly Notices of the Royal Astronomical Society*, 364(4):1105–1134, Dec 2005.

A. Stacy and V. Bromm. The First Stars: A Low-mass Formation Mode. *Astrophysical Journal*, 785:73, April 2014.

A. Stacy, T. H. Greif, and V. Bromm. The first stars: formation of binaries and small multiple systems. *Monthly Notices of the Royal Astronomical Society*, 403:45–60, March 2010.

A. Stacy, V. Bromm, and A. Loeb. Rotation speed of the first stars. *Monthly Notices of the Royal Astronomical Society*, 413:543–553, May 2011.

A. Stacy, T. H. Greif, and V. Bromm. The first stars: mass growth under protostellar feedback. *Monthly Notices of the Royal Astronomical Society*, 422:290–309, May 2012.

A. Stacy, A. H. Pawlik, V. Bromm, and A. Loeb. The mutual interaction between Population III stars and self-annihilating dark matter. *Monthly Notices of the Royal Astronomical Society*, 441:822–836, June 2014.

A. Stacy, V. Bromm, and A. T. Lee. Building up the Population III initial mass function from cosmological initial conditions. *Monthly Notices of the Royal Astronomical Society*, 462:1307–1328, October 2016.

S. W. Stahler, F. Palla, and E. E. Salpeter. Primordial stellar evolution - The pre-main-sequence phase. *Astrophysical Journal*, 308:697–705, September 1986.

P. C. Stancil, S. Lepp, and A. Dalgarno. The Deuterium Chemistry of the Early Universe. *Astrophysical Journal*, 509:1–10, December 1998.

M. Stenrup, Å. Larson, and N. Elander. Mutual neutralization in low energy Hˆ+ + Hˆ- collisions. *arXiv e-prints*, February 2009.

S. Sur, D. R. G. Schleicher, R. Banerjee, C. Federrath, and R. S. Klessen. The Generation of Strong Magnetic Fields During the Formation of the First Stars. *Astrophysical Journal, Letters*, 721:L134–L138, October 2010.

S. Sur, L. Pan, and E. Scannapieco. Mixing in Magnetized Turbulent Media. *Astrophysical Journal*, 784:94, April 2014.

H. Susa, K. Hasegawa, and N. Tominaga. The Mass Spectrum of the First Stars. *Astrophysical Journal*, 792:32, September 2014.

H. Susa. The Mass of the First Stars. *Astrophysical Journal*, 773:185, August 2013.

R. S. Sutherland and M. A. Dopita. Young oxygen-rich supernova remnants. 1: Observations of three southern remnants. *Astrophysical Journal*, 439:365–380, January 1995.

K.-i. Tadaki, D. Iono, B. Hatsukade, K. Kohno, M. M. Lee, Y. Matsuda, T. Michiyama, K. Nakanishi, T. Nagao, T. Saito, Y. Tamura, J. Ueda, and H. Umehata. CNO Emission of an Unlensed Submillimeter Galaxy at z=4.3. *Astrophysical Journal*, 876:1, May 2019.

T. Tanaka and Z. Haiman. The Assembly of Supermassive Black Holes at High Redshifts. *Astrophysical Journal*, 696:1798–1822, May 2009.

A. F. Teklu, R.-S. Remus, K. Dolag, A. M. Beck, A. Burkert, A. S. Schmidt, F. Schulze, and L. K. Steinborn. Connecting Angular Momentum and Galactic Dynamics: The Complex Interplay between Spin, Mass, and Morphology. *Astrophysical Journal*, 812:29, October 2015.

K. Tomida, K. Tomisaka, T. Matsumoto, Y. Hori, S. Okuzumi, M. N. Machida, and K. Saigo. Radiation Magnetohydrodynamic Simulations of Protostellar Collapse: Protostellar Core Formation. *Astrophysical Journal*, 763:6, January 2013.

J. K. Truelove, R. I. Klein, C. F. McKee, J. H. Holliman, II, L. H. Howell, and J. A. Greenough. The Jeans Condition: A New Constraint on Spatial Resolution in Simulations of Isothermal Self-gravitational Hydrodynamics. *Astrophysical Journal, Letters*, 489:L179–L183, November 1997.

D. Tseliakhovich and C. Hirata. Relative velocity of dark matter and baryonic fluids and the formation of the first structures. , 82(8):083520, October 2010.

M. J. Turk, T. Abel, and B. O'Shea. The Formation of Population III Binaries from Cosmological Initial Conditions. *Science*, 325:601, July 2009.

M. J. Turk, J. S. Oishi, T. Abel, and G. L. Bryan. Magnetic Fields in Population III Star Formation. *Astrophysical Journal*, 745:154, February 2012.

D. A. Verner and G. J. Ferland. Atomic Data for Astrophysics. I. Radiative Recombination Rates for H-like, He-like, Li-like, and Na-like Ions over a Broad Range of Temperature. *Astrophysical Journal, Supplement*, 103:467, April 1996.

M. Vogelsberger, S. Genel, D. Sijacki, P. Torrey, V. Springel, and L. Hernquist. A model for cosmological simulations of galaxy formation physics. *Monthly Notices of the Royal Astronomical Society*, 436:3031–3067, December 2013.

K. Waagan, C. Federrath, and C. Klingenberg. A robust numerical scheme for highly compressible magnetohydrodynamics: Nonlinear stability, implementation and tests. *Journal of Computational Physics*, 230:3331–3351, May 2011.

P. Wang, Z.-Y. Li, T. Abel, and F. Nakamura. Outflow Feedback Regulated Massive Star Formation in Parsec-Scale Cluster-Forming Clumps. *Astrophysical Journal*, 709:27–41, January 2010.

W. E. Wilson, R. H. Ferris, P. Axtens, A. Brown, E. Davis, G. Hampson, M. Leach, P. Roberts, S. Saunders, B. S. Koribalski, J. L. Caswell, E. Lenc, J. Stevens, M. A. Voronkov, M. H. Wieringa, K. Brooks, P. G. Edwards, R. D. Ekers, B. Emonts, L. Hindson, S. Johnston, S. T. Maddison, E. K. Mahony, S. S. Malu, M. Massardi, M. Y. Mao, D. McConnell, R. P. Norris, D. Schnitzeler, R. Subrahmanyan, J. S. Urquhart, M. A. Thompson, and R. M. Wark. The Australia Telescope Compact Array Broad-band Backend: description and first results. *Monthly Notices of the Royal Astronomical Society*, 416:832–856, September 2011.

J. Wolcott-Green, Z. Haiman, and G. L. Bryan. Photodissociation of H_2 in protogalaxies: modelling self-shielding in three-dimensional simulations. *Monthly Notices of the Royal Astronomical Society*, 418:838–852, December 2011.

Y. Wu, Y. Wei, M. Zhao, Y. Shi, W. Yu, S. Qin, and M. Huang. A study of high velocity molecular outflows with an up-to-date sample. *Astronomy and Astrophysics*, 426:503–515, Nov 2004.

H. Xu, J. H. Wise, M. L. Norman, K. Ahn, and B. W. O'Shea. Galaxy Properties and UV Escape Fractions during the Epoch of Reionization: Results from the Renaissance Simulations. *Astrophysical Journal*, 833:84, December 2016.

N. Yoshida, K. Omukai, L. Hernquist, and T. Abel. Formation of Primordial Stars in a ΛCDM Universe. *Astrophysical Journal*, 652:6–25, November 2006.

6.0 APPENDIX A - ADIABATIC INDEX OF H_2

In this appendix, I describe the mathematical formulation required to calculate the degrees of freedom and adiabatic index for H_2 as a function of temperature. This formulation is derived by considering the level population of para and ortho H_2 from statistical mechanics. The relation between mass fraction ($x_{\rm s}$) and number density ($n_{\rm s}$) of a species 's' is:

$$n_{\rm s} = \frac{x_{\rm s}\rho}{A_{\rm s}m} \tag{6.1}$$

where ρ is the volume density of the system and $A_{\rm s}$ is the mass number of the species s. The adiabatic index for the system can be written as a ratio of the specific heats at constant pressure ($C_{\rm p}$) to that at constant volume ($C_{\rm v}$):

$$\gamma_{\rm net} = \frac{C_p}{C_v} = \frac{c_p/k_{\rm B}}{c_v/k_{\rm B}} = \frac{c_v/k_{\rm B}+1}{c_v/k_{\rm B}} \tag{6.2}$$

where $k_{\rm B}$ is the Boltzmann constant. To do this, one first finds the specific internal energy as

$$e_{\rm g} = n_{\rm H_2} k_{\rm B} T \frac{{\rm d}\ln z}{{\rm d}\ln T} \tag{6.3}$$

where $n_{\rm H_2}$ is the column density of H_2 , T is the temperature and z is the ensemble partition function given by considering independent contributions from the translational, rotational and vibrational degrees of freedom: $z = Z_{\rm trans} Z_{\rm rot} Z_{\rm vib}$. Using $e_{\rm g}$, one then obtains the specific heat at constant volume as

$$\frac{c_v}{k_B} = \frac{1}{n_{\rm H_2}}\frac{\partial e_{\rm g}}{\partial T} \tag{6.4}$$

Using the ortho and para H_2 ($Z_{\rm rot} = Z_{\rm pH_2} Z_{\rm oH_2}$, defined in subsections below), this becomes (Krumholz, 2014):

$$\begin{aligned}\frac{c_v}{k_{\rm B}} = \frac{3}{2} + x_{\rm pH_2}\frac{\partial}{\partial T}\left(\frac{T^2}{Z_{\rm pH_2}}\frac{\partial Z_{\rm pH_2}}{\partial T}\right) + x_{\rm oH_2}\frac{\partial}{\partial T}\left(\frac{T^2}{Z_{\rm oH_2}}\frac{\partial Z_{\rm oH_2}}{\partial T}\right) \\ +(x_{\rm oH_2}+x_{\rm pH_2})\frac{\theta_{\rm vib}^2\exp(-\theta_{\rm vib}/T)}{T^2[1-\exp(-\theta_{\rm vib}/T)]^2}\end{aligned} \tag{6.5}$$

where $x_{\rm H_2} = x_{\rm oH_2} + x_{\rm pH_2}$. We will use a fixed ortho:para ratio of 3:1 (Glover and Abel, 2008), so $x_{\rm oH_2} = (3/4)x_{\rm H_2}$ and $x_{\rm pH_2} = (1/4)x_{\rm H_2}$. The last term in equation 5 corresponds to vibrational degrees of freedom of H_2, where $\theta_{\rm vib} = 5984$ K (Black and Bodenheimer, 1975).

The rotational partition function of para-H_2 is given by

$$Z_{\rm pH_2} = \sum_{J\,{\rm even}} (2J+1)\exp\left[-\frac{J(J+1)\theta_{\rm rot}}{T}\right] \tag{6.6}$$

where $\theta_{\rm rot} = 85.4$ K. Now,

$$\frac{\partial Z_{\rm pH_2}}{\partial T} = \sum_{J\,{\rm even}} \frac{J(J+1)\theta_{\rm rot}}{T^2}(2J+1)\exp\left[-\frac{J(J+1)\theta_{\rm rot}}{T}\right] \tag{6.7}$$

$$\frac{T^2}{Z_{\mathrm{pH_2}}}\frac{\partial Z_{\mathrm{pH_2}}}{\partial T} = \frac{\sum_{J\,\mathrm{even}} J(J+1)\theta_{\mathrm{rot}}(2J+1)\exp\left[-\frac{J(J+1)\theta_{\mathrm{rot}}}{T}\right]}{\sum_{J\,\mathrm{even}}(2J+1)\exp\left[-\frac{J(J+1)\theta_{\mathrm{rot}}}{T}\right]} = \frac{N_{\mathrm{pH_2}}}{Z_{\mathrm{pH_2}}} \tag{6.8}$$

$$\begin{aligned}\frac{\partial}{\partial T}\left(\frac{T^2}{Z_{\mathrm{pH_2}}}\frac{\partial Z_{\mathrm{pH_2}}}{\partial T}\right) = \Bigg[Z_{\mathrm{pH_2}}\Bigg(\sum_{J\,\mathrm{even}} J^2(J+1)^2(\theta_{\mathrm{rot}}/T)^2(2J+1)\exp\left[-\frac{J(J+1)\theta_{\mathrm{rot}}}{T}\right]\Bigg) \\ -N_{\mathrm{pH_2}}\frac{\partial Z_{\mathrm{pH_2}}}{\partial T}\Bigg]/Z^2_{\mathrm{pH_2}}\end{aligned} \tag{6.9}$$

The rotational partition function of ortho-H_2 is given by

$$Z_{\mathrm{oH_2}} = \left(\sum_{J\,\mathrm{odd}} 3(2J+1)\exp\left[-\frac{J(J+1)\theta_{\mathrm{rot}}}{T}\right]\right)\times\exp(2\theta_{\mathrm{rot}}/T) \tag{6.10}$$

where the extra exponential term in ortho Hydrogen partition functions ensures that rotation only contributes to internal energy when the rotational states are excited (Boley *et al.*, 2007; Tomida *et al.*, 2013).

$$\begin{aligned}\frac{\partial Z_{\mathrm{oH_2}}}{\partial T} = \exp(2\theta_{\mathrm{rot}}/T)\left(\sum_{J\,\mathrm{odd}} 3(2J+1)J(J+1)(\theta_{\mathrm{rot}}/T^2)\exp\left[-\frac{J(J+1)\theta_{\mathrm{rot}}}{T}\right]\right) \\ -\frac{2\theta_{\mathrm{rot}}}{T^2}\exp(2\theta_{\mathrm{rot}}/T)\left(\sum_{J\,\mathrm{odd}} 3(2J+1)\exp\left[-\frac{J(J+1)\theta_{\mathrm{rot}}}{T}\right]\right)\end{aligned} \tag{6.11}$$

$$\begin{aligned}\frac{T^2}{Z_{\mathrm{oH_2}}}\frac{\partial Z_{\mathrm{oH_2}}}{\partial T} &= \Bigg[\exp(2\theta_{\mathrm{rot}}/T)\left(\sum_{J\,\mathrm{odd}} 3(2J+1)J(J+1)\theta_{\mathrm{rot}}\exp\left[-\frac{J(J+1)\theta_{\mathrm{rot}}}{T}\right]\right) \\ &\quad -2\theta_{\mathrm{rot}}\exp(2\theta_{\mathrm{rot}}/T)\left(\sum_{J\,\mathrm{odd}} 3(2J+1)\exp\left[-\frac{J(J+1)\theta_{\mathrm{rot}}}{T}\right]\right)\Bigg]/Z_{\mathrm{oH_2}} \\ &= \frac{N_{\mathrm{oH_2}} - M_{\mathrm{oH_2}}}{Z_{\mathrm{oH_2}}}\end{aligned} \tag{6.12}$$

I first calculate the partial derivatives of $N_{\mathrm{oH_2}}$ and $M_{\mathrm{oH_2}}$ separately.

$$\begin{aligned}\frac{\partial N_{\mathrm{oH_2}}}{\partial T} = \exp(2\theta_{\mathrm{rot}}/T)\left(\sum_{J\,\mathrm{odd}} 3(2J+1)J^2(J+1)^2(\theta_{\mathrm{rot}}/T)^2\exp\left[-\frac{J(J+1)\theta_{\mathrm{rot}}}{T}\right]\right) \\ -\frac{2\theta_{\mathrm{rot}}}{T^2}\exp(2\theta_{\mathrm{rot}}/T)\left(\sum_{J\,\mathrm{odd}} 3(2J+1)J(J+1)\theta_{\mathrm{rot}}\exp\left[-\frac{J(J+1)\theta_{\mathrm{rot}}}{T}\right]\right)\end{aligned} \tag{6.13}$$

$$\begin{aligned}\frac{\partial M_{\mathrm{oH_2}}}{\partial T} = 2\theta_{\mathrm{rot}}\exp(2\theta_{\mathrm{rot}}/T)\left(\sum_{J\,\mathrm{odd}} 3(2J+1)J(J+1)(\theta_{\mathrm{rot}}/T^2)\exp\left[-\frac{J(J+1)\theta_{\mathrm{rot}}}{T}\right]\right) \\ -\left(\frac{2\theta_{\mathrm{rot}}}{T}\right)^2\exp(2\theta_{\mathrm{rot}}/T)\left(\sum_{J\,\mathrm{odd}} 3(2J+1)\exp\left[-\frac{J(J+1)\theta_{\mathrm{rot}}}{T}\right]\right)\end{aligned} \tag{6.14}$$

Then, I combine them below

$$\frac{\partial}{\partial T}\left(\frac{T^2}{Z_{\mathrm{oH_2}}}\frac{\partial Z_{\mathrm{oH_2}}}{\partial T}\right) = \frac{Z_{\mathrm{oH_2}}(\frac{\partial N_{\mathrm{oH_2}}}{\partial T} - \frac{\partial M_{\mathrm{oH_2}}}{\partial T}) - (N_{\mathrm{oH_2}} - M_{\mathrm{oH_2}})\frac{\partial Z_{\mathrm{oH_2}}}{\partial T}}{Z^2_{\mathrm{oH_2}}} \tag{6.15}$$

Now, all these equations can be used in equation (5) to find c_v/k_{B} which can then be used to find γ_{net} from equation (2).